

# The Genetic Basis of Natural Variation in *Caenorhabditis elegans* Telomere Length

Daniel E. Cook,<sup>\*,†</sup> Stefan Zdraljevic,<sup>\*,†</sup> Robyn E. Tanny,<sup>\*</sup> Beomseok Seo,<sup>‡</sup> David D. Riccardi,<sup>§,¶¶</sup>  
 Luke M. Noble,<sup>§,¶¶</sup> Matthew V. Rockman,<sup>§,¶¶</sup> Mark J. Alkema,<sup>††</sup> Christian Braendle,<sup>††</sup> Jan E. Kammenga,<sup>§§</sup>  
 John Wang,<sup>\*\*\*</sup> Leonid Kruglyak,<sup>†††,\*\*\*</sup> Marie-Anne Félix,<sup>§§§</sup> Junho Lee,<sup>\*,\*\*\*\*</sup> and  
 Erik C. Andersen<sup>\*,††††,\*\*\*\*,§§§§,1</sup>

<sup>\*</sup>Department of Molecular Biosciences, <sup>†</sup>Interdisciplinary Biological Science Program, <sup>††††</sup>Robert H. Lurie Comprehensive Cancer Center, <sup>††††</sup>Chemistry of Life Processes Institute, and <sup>§§§§</sup>Northwestern Institute on Complex Systems, Northwestern University, Evanston, Illinois 60208, <sup>‡</sup>Department of Biological Sciences, Institute of Molecular Biology and Genetics, Seoul National University, 08826, Korea, <sup>§</sup>Department of Biology, and <sup>¶¶</sup>Center for Genomics and Systems Biology, New York University, New York 10003, <sup>††</sup>Department of Neurobiology, University of Massachusetts Medical School, Worcester, Massachusetts 01605, <sup>††</sup>Centre National de la Recherche Scientifique, Institut National de la Santé et de la Recherche Médicale, Institut de Biologie Valrose, Université Nice Sophia Antipolis, 06100 Nice, France, <sup>§§</sup>Laboratory of Nematology, Wageningen University, 6708 PB, Netherlands, <sup>\*\*\*</sup>Biodiversity Research Center, Academia Sinica, Taipei 115, Taiwan, <sup>†††</sup>Departments of Human Genetics and Biological Chemistry, University of California, Los Angeles, California 90095, <sup>†††</sup>Howard Hughes Medical Institute, Chevy Chase, Maryland 20815, <sup>§§§</sup>Institut de Biologie de l'École Normale Supérieure, Centre National de la Recherche Scientifique, Institut National de la Santé et de la Recherche Médicale, 75005 Paris, France, and <sup>\*\*\*\*</sup>Department of Biophysics and Chemical Biology, Seoul National University, 08826, Korea

ORCID IDs: 0000-0003-3347-562X (D.E.C.); 0000-0003-2883-4616 (S.Z.); 0000-0001-6492-8906 (M.V.R.); 0000-0003-0229-9651 (E.C.A.)

**ABSTRACT** Telomeres are involved in the maintenance of chromosomes and the prevention of genome instability. Despite this central importance, significant variation in telomere length has been observed in a variety of organisms. The genetic determinants of telomere-length variation and their effects on organismal fitness are largely unexplored. Here, we describe natural variation in telomere length across the *Caenorhabditis elegans* species. We identify a large-effect variant that contributes to differences in telomere length. The variant alters the conserved oligonucleotide/oligosaccharide-binding fold of protection of telomeres 2 (POT-2), a homolog of a human telomere-capping shelterin complex subunit. Mutations within this domain likely reduce the ability of POT-2 to bind telomeric DNA, thereby increasing telomere length. We find that telomere-length variation does not correlate with offspring production or longevity in *C. elegans* wild isolates, suggesting that naturally long telomeres play a limited role in modifying fitness phenotypes in *C. elegans*.

**KEYWORDS** *Caenorhabditis elegans*; QTL; shelterin; telomere length; whole-genome sequence

**G**ENOME-WIDE association (GWA) studies, in which phenotypic differences are correlated with genome-wide variation in populations, offer a powerful approach to understand the genetic basis of complex traits (McCarthy *et al.* 2008). GWA requires accurate and quantitative measure-

ment of traits for a large number of individuals. Even in organisms that are studied easily in the laboratory, the measurement of quantitative traits is difficult and expensive. By contrast, the rapid decrease in sequencing costs has made the collection of genome-wide variation accessible. From *Drosophila* (Mackay *et al.* 2012; Lack *et al.* 2015) to *Arabidopsis* (Weigel and Mott 2009) to humans (The 1000 Genomes Project Consortium 2012), the whole genomes from large populations of individuals can be analyzed to identify natural variation that is correlated with quantitative traits. Because the genome itself can vary across populations, whole-genome sequence data sets can be mined for traits without measuring the physical organism. Specifically, large numbers of sequence reads generated from individuals in a

Copyright © 2016 by the Genetics Society of America

doi: 10.1534/genetics.116.191148

Manuscript received May 1, 2016; accepted for publication July 14, 2016; published Early Online July 21, 2016.

Available freely online through the author-supported open access option.

Supplemental material is available online at [www.genetics.org/lookup/suppl/doi:10.1534/genetics.116.191148/-/DC1](http://www.genetics.org/lookup/suppl/doi:10.1534/genetics.116.191148/-/DC1).

<sup>1</sup>Corresponding author: Department of Molecular Biosciences, Northwestern University, 2205 Tech Dr., Evanston, IL 60208. E-mail: erik.andersen@northwestern.edu

species can be analyzed to determine attributes of genomes, including mitochondrial- or ribosomal-DNA copy numbers. Another such trait is the length of the highly repetitive structures at the ends of linear chromosomes called telomeres (Blackburn 1991).

Telomeres are nucleoprotein complexes that serve as protective capping structures to prevent chromosomal degradation and fusion (O'Sullivan and Karlseder 2010). The DNA component of telomeres in most organisms consists of long stretches of nucleotide repeats that terminate in a single-stranded 3' overhang (McEachern *et al.* 2000). The addition of telomeric repeats is necessary because DNA polymerase is unable to completely replicate the lagging strand (Watson 1972; Levy *et al.* 1992). The length of telomeres can differ among cell populations (Samassekou *et al.* 2010), from organism to organism (Fulcher *et al.* 2014), and within proliferating cellular lineages (Frenck *et al.* 1998). Two antagonistic pathways regulate telomere length. In the first pathway, the reverse transcriptase telomerase adds *de novo* telomeric repeats to the 3' ends of chromosomes. In the second, telomere lengthening is inhibited by the shelterin complex. Shelterin forms a protective cap at telomere ends, presumably through the formation of lariat structures known as t-loops (Griffith *et al.* 1999). The t-loops are hypothesized to inhibit telomerase activity by preventing access to the 3' tail. Additionally, because uncapped telomeres resemble double-stranded DNA breaks, shelterin association with telomeric DNA represses endogenous DNA-damage repair pathways, preventing chromosomal fusion events, and preserving genome integrity (De Lange 2010).

Variation in telomere length has important biological implications. In cells lacking telomerase, chromosome ends become shorter with every cell division, which eventually triggers cell-cycle arrest (Harley *et al.* 1992). In this way, telomere length sets the replicative potential of cells and acts as an important tumor-suppressor mechanism (Harley *et al.* 1992; Deng *et al.* 2008). In populations of nonclonal human leukocytes, telomere lengths have been shown to be highly heritable (Broer *et al.* 2013). Quantitative trait loci (QTL) identified from human GWA studies of telomere length implicate telomere-associated genes, including telomerase (*TERT*), its RNA template (*TERC*), and *OBFC1* (Levy *et al.* 2010; Jones *et al.* 2012; Codd *et al.* 2013). QTL underlying variation in telomere length have been identified in *Arabidopsis thaliana*, *Saccharomyces paradoxus*, and *S. cerevisiae* using both linkage and association approaches (Gatbonton *et al.* 2006; Liti *et al.* 2009; Kwan *et al.* 2011; Fulcher *et al.* 2014). In *S. paradoxus*, natural variation in telomere lengths is mediated by differences in telomerase complex components. In *S. cerevisiae*, natural telomere lengthening is caused by a loss of an amino acid permease gene. Thus far, no studies in multicellular animals or plants have been able to identify specific genes responsible for population telomere-length differences. Recent advances in wild-strain genotypes and sequences (Andersen *et al.* 2012) in *Caenorhabditis elegans* make it a powerful model to address natural variation in telomere length and its fitness consequences.

Like in humans, telomerase and shelterin activities regulate *C. elegans* telomere length (Malik *et al.* 2000; Cheung *et al.* 2006; Meier *et al.* 2006; Shtessel *et al.* 2013). The TRT-1-containing telomerase complex is hypothesized to add TTAGGC repeats to the ends of chromosomes and prevents chromosome shortening (Meier *et al.* 2006), and the shelterin complex regulates access of the telomerase complex to chromosome ends (Raices *et al.* 2008; Cheng *et al.* 2012; Shtessel *et al.* 2013). The length of telomeres in the laboratory strain N2 is variable and ranges between 2 and 9 kb (Wicky *et al.* 1996; Raices *et al.* 2005). The telomere lengths in wild isolates of *C. elegans* are largely unexplored. Previous studies examined variation in telomere length using a small number of wild strains (Cheung *et al.* 2004; Raices *et al.* 2005). However, several of the supposed wild strains have since been determined to be mislabeled versions of the laboratory strain N2 (McGrath *et al.* 2009). Thus, it is not known if and how telomere lengths vary among *C. elegans* natural strains. Additionally, the fitness consequences of telomere-length variation have not been defined.

Here, we collected a new set of whole-genome sequences from 208 wild *C. elegans* strains and used these strains to investigate natural variation in telomere length across the species. Computational estimates of telomere lengths were confirmed using molecular measurements, indicating that this technique can be applied across a large number of wild strains. Using association mapping, we found that variation in the gene *protection of telomeres 2* (*pot-2*) is correlated with differences in *C. elegans* telomere lengths. Natural variation in *pot-2* affects gene function and causes longer than average telomeres in some wild strains. Additionally, we examined whether population differences in telomere length connect to differences in fitness traits, including brood size and longevity. Our results indicate that variation in *pot-2* does not correspond to variation in fitness as measured in the laboratory and does not show strong signatures of selection in nature. These data suggest that telomere length beyond a basal threshold is of limited consequence to *C. elegans*. Our results underscore how traits obtained from sequence data can be used to understand the dynamic nature of genomes within populations.

## Materials and Methods

### Strains

*C. elegans* strains were cultured using bacterial strain OP50 on a modified nematode growth medium [NGM with 1% agar, 0.7% agarose (NGMA)] to prevent burrowing of wild isolates (Andersen *et al.* 2014). Strain information is listed in Supplemental Material, File S1. The following strains were scored for the molecular telomere assays described below: AB4 (CB4858 isotype), CB4856, CX11285, CX11292, DL238, ECA248, ED3012, EG4349, JT11398, JU311, JU1400, JU2007, KR314, N2, NIC2, NIC3, NIC207, PB303, and QX1212.

### Library construction and sequence acquisition

DNA was isolated from 100–300  $\mu$ l of packed animals using the Blood and Tissue DNA isolation kit (QIAGEN, Valencia, CA). The provided protocol was followed with the addition of RNase (4  $\mu$ l of 100 mg/ml) following the initial lysis for 2 min at room temperature (RT). DNA concentration was determined using the Qubit dsDNA Broad Range Assay Kit (Invitrogen, Carlsbad, CA). Libraries were generated using the Illumina Nextera Sample Prep Kit and indexed using the Nextera Index Kit. A total of 24 uniquely-indexed samples were pooled by mixing 100 ng of each sample. The pooled material was size selected by electrophoresing the DNA on a 2% agarose gel and excising the fragments ranging from 300 to 500 bp. The sample was purified using the QIAGEN MinElute Kit and eluted in 11  $\mu$ l of Buffer EB. The concentration of the purified sample was determined using the Qubit dsDNA High Sensitivity Assay Kit. Sequencing was performed on the Illumina HiSeq 2500 platform. To increase coverage of some strains, we incorporated data from two separate studies of wild strains (Thompson *et al.* 2013; Noble *et al.* 2015).

### Trimming and demultiplexing

When necessary, demultiplexing and sequence trimming were performed using `fastx_barcode_splitter.pl` (version 0.0.14) (Gordon and Hannon 2010). Sequences were trimmed using `trimmomatic` (version 0.32) (Bolger *et al.* 2014). Nextera libraries were trimmed using the following parameters:

```
NexteraPE-PE.fa:2:80:10 MINLEN:45
```

TruSeq libraries were trimmed using:

```
TruSeq2-PE.fa:2:80:10 TRAILING:30 SLIDINGWINDOW:4:30  
MINLEN:30
```

The full details of the preparation, source, and library are available in File S2.

### Alignment, variant calling, and filtering

FASTQ sequence data has been deposited under National Center for Biotechnology Information Bioproject accession PRJNA318647. Sequences were aligned to WS245 (<http://www.wormbase.org>) using the Burrows–Wheeler Aligner (BWA) (version 0.7.8-r455) (Li and Durbin 2009). Optical/PCR duplicates were marked with PICARD (version 1.111). BAM and CRAM files are available at <http://www.elegansvariation.org/Data>. To determine which type of single-nucleotide-variant (SNV) caller would perform best on our dataset and to set appropriate filters, we simulated variation in the N2 background. We used `bamsurgeon` (<http://github.com/adamewing/bamsurgeon>), which modifies base calls to simulate variants at specific positions within aligned reads and then realigns reads to the reference genome using BWA. We simulated 100,000 SNVs in 10 independent simulation sets. Of the 100,000 sites chosen in each simulation set, `bamsurgeon` successfully inserted an average of 95,172 SNVs. Using these 10 simulated variant sets, we tested two different methods of grouping our strains for variant calling:

calling strains individually (comparing sequences from a single strain to the reference) or calling strains jointly (comparing all strains in a population to each other). After grouping, `bcftools` has two different calling methods: a consensus caller (specified using `-c`), and a more recently developed multi-allelic caller (specified using `-m`) (Li 2011). We performed variant calling using all four combinations of individual/joint calling and the consensus/multi-allelic parameters. Because of the hermaphroditic life cycle of *C. elegans*, heterozygosity rates are likely low. Occasionally, heterozygous variants will be called despite skewed read support for reference or alternative alleles. To account for these likely erroneous calls, we performed ‘heterozygous polarization’ using the log-likelihood ratios of reference to alternative genotype calls. When the log-likelihood ratio was  $< -2$  or  $> 2$ , heterozygous genotypes were polarized (or switched) to reference genotypes or alternative genotypes, respectively. All other SNVs with likelihood ratios between  $-2$  and  $2$  were called NA. Following variant calling and heterozygous polarization on resulting calls, we observed increased rates of heterozygous calls using joint methods and decreased true positive (TP) rates using our simulation data set (File S3, File S4). Given *C. elegans*’ predominantly self-fertilizing mode of reproduction, we decided to focus on the individual-based calling method that performed better. Next, we determined the optimal filters to maximize TP rates and minimize false positive (FP) and false negative (FN) results using our simulated data (File S4). After implementing different combinations of filters, we found that depth (DP), mapping quality (MQ), variant quality (QUAL), and the ratio of high-quality alternative base calls (DV) over DP filters worked well (Figure S1). Variants with  $DP \leq 10$ ,  $MQ \leq 40$ ,  $QUAL < 30$ , and  $DV/DP < 0.5$  were called NA. Using these filters, we called 1.3-million SNVs across 152 isotypes. This data set is available at <http://www.andersenlab.org/Research/Data/Cooketal>.

### Validation of SNV-calling methods

In addition to performing simulations to optimize SNV-calling filters, we compared our whole-genome sequence variant calls with SNVs identified previously in CB4856 (Wicks *et al.* 2001). Out of 4256 sites we were able to call in regions that were sequenced using Sanger sequencing, we correctly identified 4223 variants (99.2% of all variants) in CB4856. One TP was erroneously filtered and two FPs were removed using our filters, and we failed to call the nonreference allele for 30 variants (FNs).

Additionally, we examined sequence variants with poor parameter values in terms of depth, quality, heterozygosity, or modification by our heterozygous polarization filter. We used primer3 (Rozen and Skaletsky 2000) to generate a pair of primers for performing PCR and a single forward primer for Sanger sequencing. We successfully sequenced 73 of 95 sites chosen from several strains. Comparison of variant calls after imputation and filtering yielded 46 TPs and 14 true negatives. We successfully removed 3 out of 11 FPs and erroneously filtered two sites that should have been called as nonreference

(FN). We also validated the variant responsible for the F68I change in JT11398.

### Identification of clonal sets

Some strains in our original collection were isolated from the same or nearly identical locations. Therefore, we determined if these strains share distinct genome-wide haplotypes or isotypes. To determine strain relatedness, we sequenced and called variants from sequencing runs independently (e.g., individual FASTQ pairs) to ensure that strains were properly labeled before and after sequencing. We then combined FASTQ files from sequencing runs for a given strain and examined the concordance among genotypes. Comparison of variants identified among sequenced strains were used to determine whether the strains carried identical haplotypes. We observed that some strains were highly related to each other as compared with the rest of the population. Strains that were >99.93% identical across 1,589,559 sites identified from sequencing runs of individual strains were classified as isotypes (Figure S2). The disparity between the final 1.3-million SNV set as compared to the 1.5-million SNV set comes from the different levels and types of filters applied for strain concordances to make isotypes or from SNV calling across the isotype population. Because LSJ1 and N2 share a genome-wide genotype but exhibit distinct phenotypes (Sterken *et al.* 2015), we treated each strain as a separate isotype. We found the following isotype differences from the previous characterization of a large number of strains (Andersen *et al.* 2012). JU360 and JU363 were previously thought to be separate, but highly related, isotypes. We found that, at the genome-wide level and at high depths of coverage, these strains are from the same isotype. Several wild strains isolated before 2000 had different genome-wide haplotypes compared to strains with the same names but stored at the *Caenorhabditis* Genetics Center (CGC). CB4851 from the CGC had a different genome-wide haplotype compared to a strain with the same name from Cambridge, United Kingdom. We renamed the CB4851 strain from the CGC as ECA243. By contrast, the version from Cambridge, United Kingdom was nearly identical to N2 and not studied further. CB4855 from the CGC has a genome-wide haplotype that matches CB4858, which has a different history and isolation location. Therefore, we cannot guarantee the fidelity of this strain, and it was not studied further. CB4855 from Cambridge, United Kingdom is different from the CGC version of CB4855. We gave this strain the name ECA248 to avoid confusion. CB4858 from CGC has a different genome-wide haplotype than CB4858 from Cambridge, United Kingdom. Therefore, we renamed CB4858 from Cambridge, United Kingdom to ECA252, and it is a separate isotype. The CB4858 from the CGC was renamed ECA251 and is the reference strain from the CB4858 isotype.

### Imputation and variant annotation

Following SNV calling and filtering, some variant sites were filtered. Next, we generated an imputed SNV set using beagle (version r1399) (Browning and Browning 2016). This imputed

variant set is available at <http://www.andersenlab.org/Research/Data/Cooketal>. We used SnpEff (version 4.1g) (Cingolani *et al.* 2012) on this SNV set to predict functional effects.

### Telomere-length estimation

Telomere lengths were estimated using TelSeq (version 0.0.1) (Ding *et al.* 2014) on BAM files derived from wild isolates or Million Mutation Project (MMP) strain sequencing. To estimate telomere lengths, TelSeq determines the reads that contain greater than seven telomeric hexamer repeats (TTAGGC for *C. elegans*). Compared to most hexamers, telomeric hexamers can be found tandemly repeated within sequenced reads. TelSeq calculates the relative proportion of reads that appear to be telomerically derived among all sequenced reads and transforms this value into a length estimate using the formula  $l = t_k \cdot s \cdot c$  where  $l$  is the length estimate and  $t_k$  is the abundance of reads with a minimum of  $k$  telomeric repeats. The value of  $s$  is the fraction of all reads with a GC composition similar to the telomeric repeat (48–52% for *C. elegans*). The value of  $c$  is a constant representing the length of 100-bp windows within the reference genome where GC content = GC content of the telomeric repeat / total number of telomere ends. By default, TelSeq provides length estimates applicable to humans. We found the number of 100-bp windows with a 50% GC content in the WS245 reference genome to be 58,087. We calculated  $c$  for *C. elegans* as 58,087 kb/12 telomeres = 484. This value was used to transform human length estimates to length estimates appropriate to *C. elegans*.

Notably, telomere-length estimates are averaged across all chromosomes, as no specific data about any one particular telomere is determined. To assess how well the TTAGGC hexamer distinguishes telomeric reads from nontelomeric reads, we examined the frequencies of noncyclical permutations of the *C. elegans* hexamer in the N2 laboratory strain using TelSeq (Figure S3). We observe that the majority of hexamers examined were not present in more than six copies in a high frequency of reads. By contrast, the reads possessing the telomeric hexamer with seven copies or more were more abundant than any other hexamer. Tandem repeats of the telomeric hexamer are present within the reference genome at the ends of each chromosome and occasionally internally within chromosomes at between 2 and 71 copies (File S5). After running TelSeq on our wild isolates, we removed eight sequencing runs (out of 868 total) that possessed zero reads with 15 or more copies of the telomeric hexamer. These sequencing runs provide additional support for SNV calling but had short read lengths that would underestimate telomere length. We used the weighted average of telomere-length estimates for all runs of a given strain based on total reads to calculate telomere-length estimates. File S6 details telomere-length estimates for every sequencing run.

### Quantitative PCR assays for telomere-length measurements

Telomere lengths were measured by quantitative PCR (qPCR) as described previously with some modifications (Cawthon



2009). Primer sequences were modified from the vertebrate telomere repeat (TTAGGG) to use the *C. elegans* telomere repeat (TTAGGC):

telG: 5'-ACACTAAGCTTTGGCTTTGGCTTTGGCTTTGGCTT  
AGTCT-3'

telC: 5'-TGTTAGGTATGCCTATGCCTATGCCTATGCCTATGCC  
TAAGA-3'

The internal control, *act-1*, was amplified using the following primer pair:

forward: 5'-GTCGGTATGGGACAGAAGGA-3'

reverse: 5'-GCTTCAGTGAGGAGGACTGG-3'

Two primer pairs were amplified separately (singleplex qPCR). All the samples were run in triplicate. qPCR was performed using iQ SYBR green supermix (Bio-Rad, Hercules, CA) with iCycler iQ real-time PCR detection system (Bio-Rad). After thermal cycling, cycle threshold ( $C_t$ ) values were exported from Bio-Rad iQ5 software.

#### **Terminal restriction fragment Southern blot assay**

Animals were grown on 100-mm petri dishes with NGM seeded with OP50. Synchronized adult animals were harvested and washed four times with M9 buffer. Pelleted animals were lysed for 4 hr at 50° in buffer containing 0.1 M Tris-Cl (pH 8.5), 0.1 M NaCl, 50 mM EDTA (pH 8.0), 1% SDS, and 0.1 mg/mL proteinase K. DNA was isolated by phenol extraction and ethanol precipitation. DNA was eluted with buffer containing 10 mM Tris (pH 7.5) and 1 mM EDTA. DNA was then treated with 10 µg/mL boiled RNase A. DNA was again isolated with phenol extraction and ethanol precipitation. *HinfI* digested 5 µg of DNA at 37° overnight. Telomere restriction fragment was blotted as described previously (Seo *et al.* 2015) (Figure S4). Digoxigenin-labeled (TTAGGC)<sub>4</sub> oligonucleotides were used as probes. Digoxigenin probes were detected with DIG Nucleic Acid Detection Kit (Hoffmann La Roche, Nutley, NJ). Blots were imaged with ImageQuant LAS4000 (GE healthcare).

#### **FISH assays**

FISH was performed as previously described (Seo *et al.* 2015). Embryos were isolated by bleaching synchronized adult animals using standard methods (Stiernagle 2006). Isolated embryos were fixed in 2% paraformaldehyde for 15 min at RT on a polylysine treated glass slide. The slide was put on dry ice and freeze-cracked. The embryos were permeabilized in ice-cold methanol and acetone for 5 min each. The slides were washed with 1× PBS containing 0.1% Tween-20 (PBST) three times for 15 min each at RT. Also added on the slide was 10 µl of hybridization buffer [50 nM Cy3-(TTAGGC)<sub>3</sub> peptide nucleic acids probe (PANAGENE), 50% formamide, 0.45 M sodium chloride, 45 mM sodium citrate, 10% dextran sulfate, 50 µg/ml heparin, 100 µg/ml yeast tRNA, 100 µg/ml salmon sperm DNA]. The samples were denatured on a heat block at 85° for 3 min. After overnight incubation at 37°, the samples were washed in the following order: 1× PBST once for 5 min at RT,

2× SSC (0.3 M sodium chloride, 30 mM sodium citrate) in 50% formamide once for 30 min at 37°, 1× PBST three times for 10 min each at RT. The samples were incubated in DAPI and mounted in antibleaching solution (Vectashield). The samples were imaged with a confocal microscope, and the distinct foci were measured for fluorescence intensity (LSM700; Carl Zeiss, Thornwood, NY). Telomere spots were quantified with TFL-TELO software (Dr. Peter Lansdorp, Terry Fox Laboratory, Vancouver, BC) (Poon *et al.* 1999). Because embryos were scored for fluorescent foci, it is possible that the telomere-length estimates were quantified from both telomeres and internal repeat elements sharing homology to telomeric DNA.

#### **GWA mapping**

GWA mapping was performed on marker genotype data and telomere-length estimates using the rrBLUP package (version 4.3) (Endelman 2011) and GWAS function. rrBLUP requires a kinship matrix and an SNV set to perform GWA. We generated a kinship matrix using our imputed SNV set with the A.mat function within rrBLUP. Genomic regions of interest were determined empirically from simulating a QTL that explained 20% of the phenotypic variance at each marker in our mapping data set. All simulated QTL were mapped within 100 markers (50 markers to the left and 50 markers to the right) of the simulated marker position. To generate a SNV set for mapping, we again used our imputed SNV set. However, we filtered the number of SNVs to a set of 38,688 markers. This set was generated by lifting over (from WS210 to WS245) a set of 41,888 SNVs previously used for GWA mapping (Andersen *et al.* 2012) and filtering our imputed SNVs to those sites.

#### **MMP analysis**

Whole-genome sequence data from mutagenized strains within the MMP was obtained from the sequence read archive (SRA) (project accession number SRP018046). We removed 59 strains that were contaminated with other strains. We were also unable to locate the sequence data for 12 MMP strains on SRA, leaving us with 1,936 mutagenized strains. Within the MMP project, read lengths varied among sequencing runs, being either 75 bp or 100 bp. We ran TelSeq on all sequencing runs assuming 100-bp reads. To use 75-bp sequencing runs, we took the 448 strains that were sequenced at both 75 and 100 bp lengths and used those estimates to develop a linear model. Then, this model was used to transform 75-bp length estimates to 100-bp estimates (Figure S5). We then used the weighted average of telomere-length estimates for all runs of a given strain based on total reads to calculate telomere-length estimates. Because telomeric reads resemble PCR duplicates, TelSeq uses them in calculating telomere length. However, we observed very low PCR and optical duplicate rates among MMP sequence data, likely due to differences in library preparation in contrast to wild isolate sequence data. These differences likely account for shorter telomere estimates from the MMP sequence data.

Long-telomere strains from the MMP were classified as strains with telomere lengths greater than the 98th quantile of

all MMP strains (6.41 kb). Mutation data were obtained from the MMP website ([http://genome.sfu.ca/mmp/mmp\\_mut\\_strains\\_data\\_Mar14.txt](http://genome.sfu.ca/mmp/mmp_mut_strains_data_Mar14.txt)). A hypergeometric test was performed to identify which genes were enriched for mutations from long-telomere strains (File S7) using the *phyper* function in R (R Development Core Team 2013). FX1400 was propagated for 10 generations prior to whole-genome sequencing. Telomere length was estimated using TelSeq.

### Statistical analyses

Statistical analyses were performed using R (version 3.2.3). Plots were produced using ggplot2 (version 2.0.0).

### Longevity assays

At least 80 L4 animals were plated onto each of three separate 6-cm NGMA plates in two independent assays and viability assessed each day until all animals were scored as dead or censored from the analysis as a result of bagging or missing animals. Animals were scored as dead in the absence of touch response and pharyngeal pumping. Animals were transferred to fresh plates every day from the initiation of the assay until day 7 of adulthood to remove progeny, and transferred every other day until the completion of the assay. The following short telomere strains were scored: EG4349, JU2007, NIC1, and NIC3. The following long-telomere strains were scored: KR314, NIC207, QX1212, and RC301. Additionally, N2 and CB4856 were scored.

### High-throughput fecundity assays

Assays were performed similarly to those previously reported (Andersen *et al.* 2015) with the following differences: Animals were bleached, synchronized, and grown to L4 larvae in 96-well plates. From the L1–L4 stage, animals were fed 5 mg/ml of a large-scale production HB101 lysate in K medium (Boyd *et al.* 2010) to provide a stereotyped and constant food source. Then, three L4 larvae from each of the 152 genotypes were dispensed using a COPAS BIOSORT instrument to wells containing 10 mg/ml HB101 lysate in K medium, and progeny were counted 96 hr later. Fecundity data were calculated using 12 samples—triplicate technical replicates from four biological replicates. The data were processed using COPASutils (Shimko and Andersen 2014) and statistically analyzed using custom R scripts.

### Clustering of relatedness

Variant data for dendrogram comparisons were assembled by constructing a FASTA file with the genome-wide variant positions across all strains and subsetting by regions as described. Multiple sequence comparison by log-expectation (MUSCLE, version v3.8.31) (Edgar 2004) was used to generate neighbor-joining trees. The R packages ape (version 3.4) (Paradis *et al.* 2004) and phyloseq (version 1.12.2) (McMurdie and Holmes 2013) were used for data processing and plotting.

### Data availability

All data necessary for confirming the conclusions presented in the article are represented fully within the article.

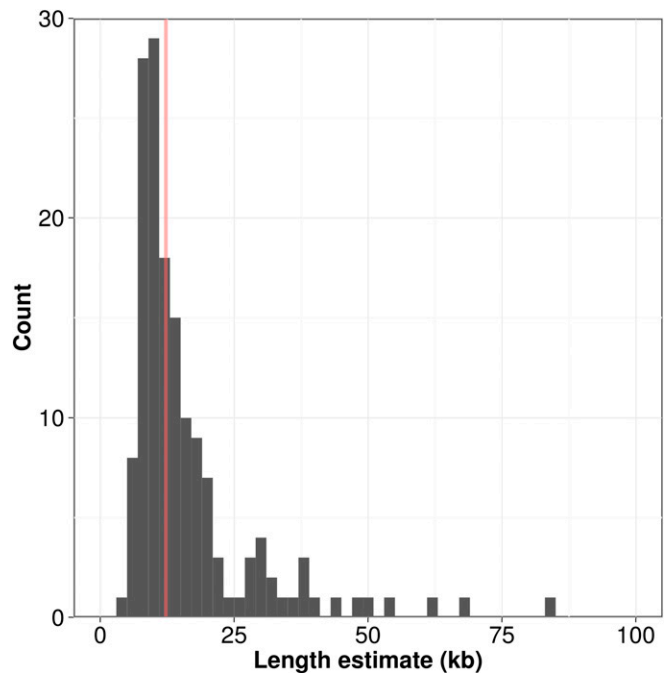


**Figure 1** Distribution of telomere-length estimates. A histogram of telomere-length estimates weighted by the number of reads sequenced per run is shown. Bin width is 2. The red line represents the median telomere-length estimate of 12.2 kb.

## Results

### Whole-genome sequencing of a large number of wild *C. elegans* strains identifies new isotypes and highly diverged strains

Previous genome-wide analyses of *C. elegans* population diversity used single-nucleotide variants (SNVs) ascertained from only two strains (Rockman and Kruglyak 2009), from reduced representation sequencing that only studied a fraction of the genome (Andersen *et al.* 2012), or from a small set of wild strains (Thompson *et al.* 2013). To address these limitations, we sequenced the whole genomes of a collection of 208 wild strains (File S1). Because *C. elegans* reproduction occurs primarily through the self-fertilization of hermaphrodites, highly related individuals proliferate and disperse, often in close proximity to one another (Barrière and Félix 2005; Félix and Braendle 2010). As a result, strains isolated in nature are frequently identical and share genome-wide haplotypes or isotypes. Sequencing data generated from strains belonging to the same isotype can be combined to increase depth of coverage and to improve downstream analyses. To identify which strains shared the same genome-wide haplotypes, we compared all of the variation identified in each of the 208 strains to each other in pairwise comparisons. The 208 strains reduce to 152 unique genome-wide haplotypes or isotypes (File S1). The combination of sequence data from all strains that make up an isotype led to a 70-fold median depth of coverage (Figure S6), enabling the discovery of SNVs and other genomic features. The number of SNVs in

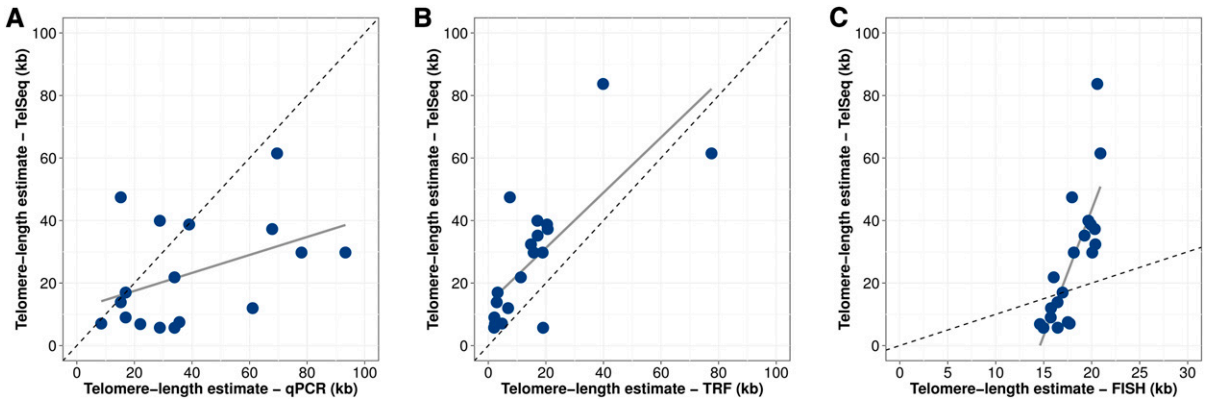


**Figure 2** Telomere-length estimates correlate with alternative molecular measurement methods. Scatterplot of TelSeq telomere-length estimates (y-axis) plotted against alternative methods of telomere-length measurement on the x-axis. Alternative methods plotted on the x-axis and their associated Spearman's rank correlation are (A) qPCR measurements normalized by N2 qPCR telomere-length estimate and scaled relative to the TelSeq N2 telomere-length estimate ( $\rho = 0.445$ ,  $P = 0.049$ ), (B) TRF ( $\rho = 0.699$ ,  $P = 8.5e^{-4}$ ), and (C) FISH measurements normalized by N2 FISH telomere-length estimate and scaled relative to the TelSeq N2 telomere-length estimate ( $\rho = 0.815$ ,  $P = 1.03e^{-5}$ ). Gray lines represent the regression lines between TelSeq and each method. Dashed diagonal lines represent identity lines.

comparisons of each isotype to the reference strain N2 ranged from strains highly similar to N2 with few SNVs, to highly diverged strains with 402,436 SNVs (Figure S7), and the density of SNVs across the genome matched previous distributions with more variants on chromosome arms than centers (Andersen *et al.* 2012) (Figure S8). An analysis of relatedness among these 152 isotypes recapitulated the general relationships previously identified among a set of 97 wild isotypes (Andersen *et al.* 2012) (Figure S9) with the addition of 55 new isotypes. Past studies identified one highly diverged strain isolated from San Francisco, CA, QX1211, which had divergence almost three times the level of other wild *C. elegans* strains (Andersen *et al.* 2012). Among the 55 new isotypes, one additional strain, ECA36 from New Zealand, is equally diverged, suggesting that wider sampling will recover additional diversity for this species. Altogether, our considerably expanded collection of whole-genome sequence data serves as a powerful tool to interrogate how natural variation gives rise to differences among individuals in a natural population.

### ***C. elegans* wild strains differ in telomere lengths**

Our collection of high-depth whole-genome sequence data samples a large number of strains in the *C. elegans* species. The recent development of TelSeq, a program designed to estimate telomere length using short-read sequence data (Ding *et al.* 2014), allowed us to examine natural variation in telomere lengths computationally across wild *C. elegans* strains. We detected considerable natural variation in the total length of telomeric DNA in a strain (Figure 1), ranging from 4.12 kb to a maximum of 83.7 kb with a median telomere length of 12.25 kb (File S8). The TelSeq telomere-length estimate for N2 from our study was 16.97 kb, which is higher than previous estimates of 4–9 kb (Wicky *et al.* 1996) and 2–9 kb (Raices *et al.* 2005). This discrepancy likely arises from computational as compared to molecular assays, as we will discuss below. We found that the distribution of telomere

lengths in the *C. elegans* population approximated a normal distribution with a right tail containing strains with longer than average telomeres. We found that our computational estimates of telomere length from Illumina sequence data were significantly influenced by library preparation, possibly driven by the method of DNA fragmentation (Figure S10). However, we were able to control for these differences using a linear model. We also observed a weak correlation between depth of coverage and TelSeq length estimates, but adjustments for library preparation eliminated this relationship (Figure S11).

TelSeq length estimates have been shown to give similar results as molecular methods to measure human telomere length (Ding *et al.* 2014). As of now, no studies have used TelSeq to examine *C. elegans* telomeres, so we investigated how well TelSeq estimates correlated with molecular methods, including terminal restriction fragment (TRF) Southern blot analyses, qPCR of telomere hexamer sequences, and FISH analyses. Using 20 strains, we found that the results from these molecular assays correlated well ( $\rho = 0.445$  TRF, 0.815 FISH, 0.699 qPCR; Spearman's rank correlation) with computational estimates of telomere lengths (Figure 2; File S9). These molecular results validated our computational estimates of telomere lengths and indicate that we can use TelSeq estimates to investigate the genetic causes underlying telomere variation.

### ***Species-wide telomere-length differences correlate with genetic variation on chromosome II***

To identify the genes that cause differences in telomere length across the *C. elegans* population, we used a GWA mapping approach as performed previously (Andersen *et al.* 2012) but taking advantage of the larger collection of wild strains. We treated our computational estimates of telomere length as a quantitative trait and identified one significant QTL on the right arm of chromosome II (Figure 3; File S10). To identify

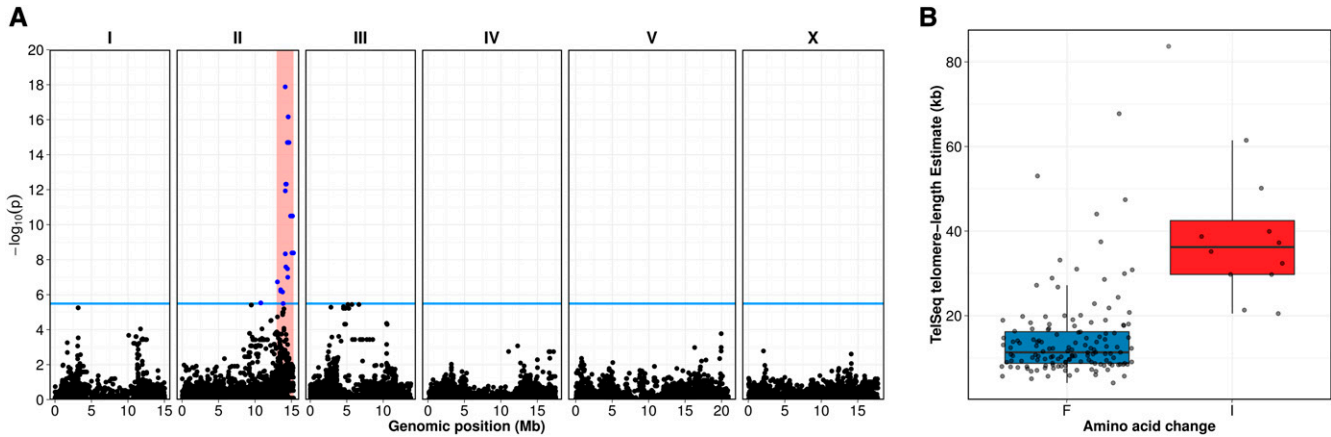


**Figure 3** GWA of telomere length. (A) GWA of telomere-length residuals (conditioned on DNA library) is visualized using a Manhattan plot. Genomic coordinates are plotted on the x-axis against the negative of the log-transformed  $P$ -value of a test of association on the y-axis. The blue bar indicates the Bonferroni-corrected significance threshold ( $\alpha = 0.05$ ). Blue points represent SNVs above the significance threshold whereas black points represent SNVs below the significance threshold. Light-red regions represent the C.I.s surrounding significantly associated peaks. (B) Shown is the split between TelSeq-estimated telomere lengths (y-axis) by genotype of *pot-2* at the presumptive causative allele as boxplots (x-axis). The variant at position 14,524,396 on chromosome II results in a putative F68I coding change. Horizontal lines within each box represent the median, and the box represents the interquartile range (IQR) from the 25th–75th percentile. Whiskers extend to  $1.5\times$  the IQR above and below the box. Points represent individual strains.

the variant gene(s) that underlie this QTL, we investigated the SNVs within a large genomic region (12.9–15.3 Mb) surrounding the most significant marker on chromosome II. This region contains 557 protein-coding genes (File S11), but only 332 of these genes contained variants that are predicted to alter the amino acid sequences among the 152 strains. We examined genes with predicted protein-coding variants that could alter telomere length by correlating their alleles with the telomere-length phenotype. Nine genes possessed variation that was most highly correlated with telomere length ( $\rho \geq 0.39$ ; File S11). The chromosome II QTL explains 28.4% of the phenotypic variation in telomere length. Three additional suggestive QTL on chromosomes I, II, and III were detected close to but below the significance threshold. Taken together, the four QTL explain 56.7% of the phenotypic variation in telomere length.

#### Variation in *pot-2* underlies differences in telomere length

One of the nine genes in the chromosome II large-effect QTL is *pot-2*, a gene that was implicated previously in the regulation of telomere length (Raices *et al.* 2008; Cheng *et al.* 2012; Shtessel *et al.* 2013). A quantitative complementation test could be used to confirm that wild strains have the same functional effect as a *pot-2* deletion. However, differences in telomere length caused by mutations in genes that encode telomere-associated proteins often do not have observable telomere defects for a number of generations (Vulliamy *et al.* 2004; Armanios *et al.* 2005; Marrone *et al.* 2005). It is technically not feasible to keep the genome heterozygous during long-term propagation. Given the large number of genes present within our confidence interval and challenges associated with examining telomere length using traditional genetic approaches, we sought alternative methods to con-

firm that variation in *pot-2* could cause long telomeres. The ability to computationally estimate telomere length allowed us to further validate our approach using data from the MMP (Thompson *et al.* 2013) and examine whether the equivalent of a mutant screen for telomere length would provide insight into our result examining wild isolate genomes.

The MMP generated >2000 mutagenized strains using the laboratory N2 background. After each strain was passaged by self-mating of hermaphrodites for 10 generations, the strains were whole-genome sequenced to identify and predict the effects of induced mutations. The MMP data set can be used to identify correlations of phenotype and mutant genes in the laboratory strain background. We obtained whole-genome sequence data from 1936 mutagenized N2 strains, each of which has a unique collection of mutations. Importantly, 10 generations of self-propagation of these mutagenized strains prior to sequencing likely allowed telomere lengths to stabilize in response to mutations in genes that regulate telomere length, enabling us to observe differences. TelSeq returned telomere-length estimates for this population, which had a right long-tailed distribution (Figure 4A). The median telomere length among the mutagenized strains was 4.94 kb, which is much shorter than the length estimate of N2 in our collection (16.97 kb). This disparity likely arises due to differences in library preparation, sequencing platform, and data processing. We classified 39 of 1936 strains within the population as long-telomere strains with telomere lengths greater than 6.41 kb (98th percentile). Reasoning that certain mutant genes would be overrepresented in these 39 strains compared to the others, we performed a hypergeometric test to identify if enrichment for particular genes in long-telomere strains existed. After adjusting for multiple statistical tests, we identified *pot-2* as the only gene highly enriched for mutations in six of the 39 long-telomere strains



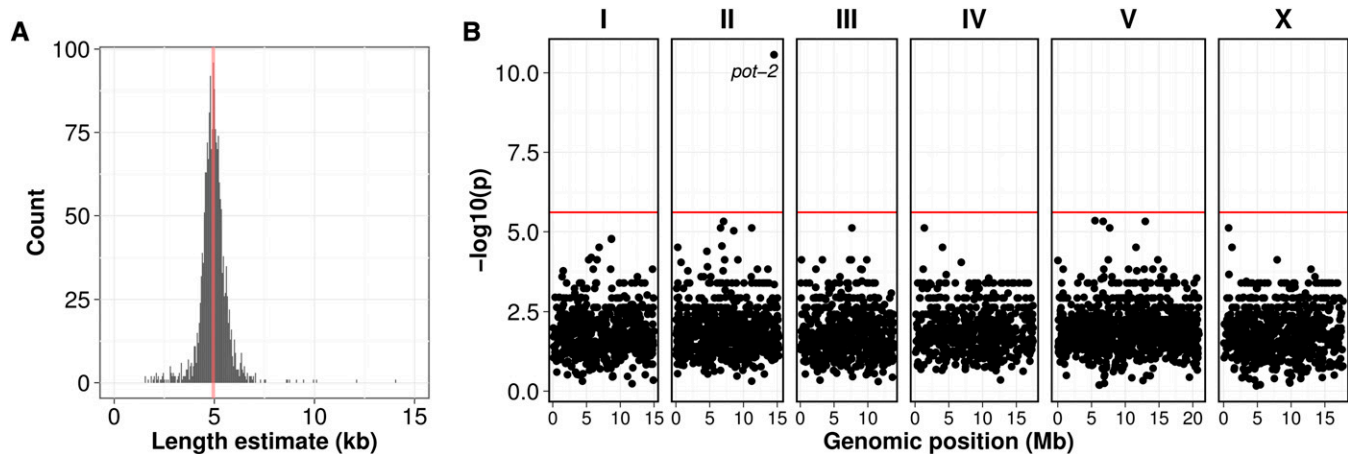


**Figure 4** Mutations in *pot-2* are more often found in strains with long telomeres than in strains with short telomeres. (A) A histogram of telomere-length estimates among the 1936 mutagenized strains from the MMP. Median telomere length is 4.94 kb. (B) Plot of significance from a hypergeometric test for every *C. elegans* protein-coding gene. The red line represents the Bonferroni ( $\alpha = 0.05$ ) threshold set using the number of protein-coding genes (20,447). Each point represents a gene plotted at its genomic position on the x-axis, and the log-transformed *P*-value testing for enrichment of mutations in long-telomere strains.

( $P = 2.69e^{-11}$ , Bonferroni corrected; Figure 4B). No other genes within any of the QTL intervals or any other part of the genome were enriched for mutations among long-telomere strains. This approach was different from association mapping and identified the same locus regulating telomere length. Additionally, we computationally examined telomere length from whole-genome sequencing of a *pot-2* knockout strain. This strain possesses a large deletion that spans the first and second exons of *pot-2*, likely rendering it nonfunctional. We propagated this mutant strain for 10 generations prior to whole-genome sequencing and TelSeq analysis. The telomere length of *pot-2(tm1400)* mutants was calculated to be 30.62 kb. Given these data, we have three independent tests that indicate that variation in *pot-2* likely underlies natural differences in telomere lengths across the *C. elegans* species.

Our results are consistent with the established role of *pot-2* as an inhibitor of telomere lengthening (Shtessel *et al.* 2013). However, no connection of *pot-2* to natural variation in telomere lengths has been described previously. We next investigated the variant sites altered in the *C. elegans* species along with the mutations found in the MMP mutagenized strains (Figure 5). We found that the natural variation in *pot-2* resulted in a putative phenylalanine-to-isoleucine (F68I) change in the OB-fold (oligonucleotide/oligosaccharide-binding fold) domain of 12 strains. OB-fold domains are involved in nucleic acid recognition (Flynn and Zou 2010), and the OB fold of the human POT-2 homolog (hPOT1) binds telomeric DNA (Lei *et al.* 2004). Strains with the POT-2(68I) allele have long telomeres on average, whereas strains with POT-2(68F) allele have normal-length telomeres on average. Synonymous variants or variation outside of the OB-fold domain were rarely found in strains with long telomeres. Because loss of *pot-2* is known to cause long telomeres (Raices *et al.* 2008; Cheng *et al.* 2012; Shtessel *et al.* 2013), the F68I variant likely reduces or eliminates the function of *pot-2*. Additionally,

six out of the 39 long-telomere MMP strains had mutations in *pot-2*, including five strains that had mutations within or directly adjacent to the OB fold and an additional strain with a nonsense mutation outside the OB-fold domain that likely destabilizes the transcript. These data support the hypothesis that *pot-2* is the causal gene underlying variation in telomere lengths across the *C. elegans* species.

#### Natural variants in *pot-2* do not have detectable fitness consequences

We connected genetic variation in the gene *pot-2* with telomere-length differences across *C. elegans* wild strains. Specifically, an F68I variant in the putative telomere-binding OB-fold domain might cause reduction of function and long telomeres. A variety of studies have observed a relationship between telomere length and organismal fitness, including longevity or cellular senescence (Harley *et al.* 1992; Heindinger *et al.* 2012; Soerensen *et al.* 2012). Our results with natural variation in telomere lengths provided a unique opportunity to connect differences in the length of telomeres with effects on organismal fitness. We measured offspring production for our collection of 152 wild strains and found no correlation with telomere length ( $\rho = 0.062$ ; Figure 6A). Long telomeres allow for increased replicative potential of cells (Harley *et al.* 1992), but it is unclear how the replicative potential of individual cells contributes to organismal longevity phenotypes (Hornsby 2007). We chose nine strains covering the range of telomere-length differences and found no correlation with longevity ( $\rho = 0.05$ ; Figure 6B, Figure S12). Taken together, these results suggest that the long telomeres found in some wild *C. elegans* strains do not have significant fitness consequences in these laboratory-based experiments.

Because we did not observe a strong effect on organismal fitness, we investigated the population genetics of *pot-2* to test whether that locus had any signature of selection.

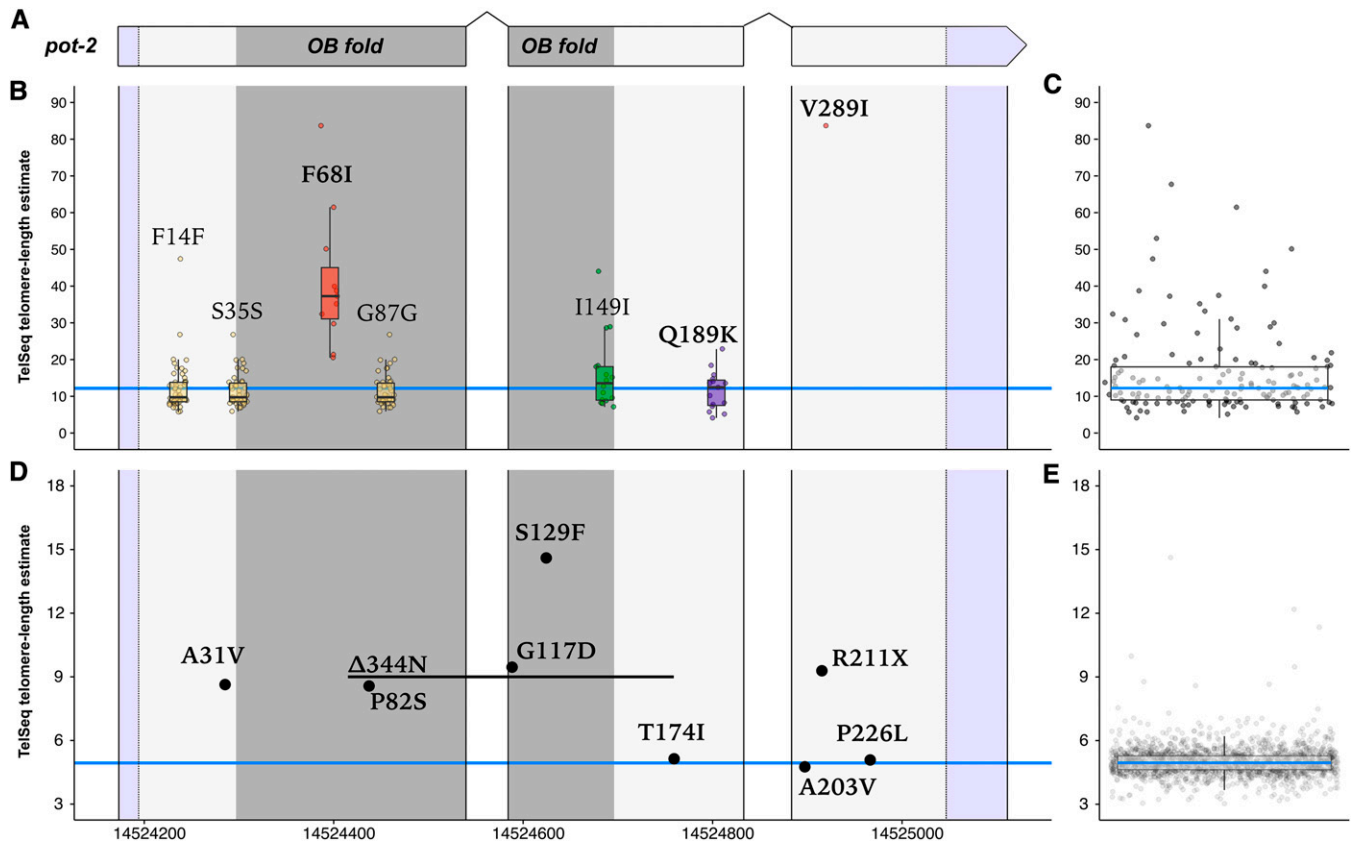


**Figure 5** Variation within *pot-2* in wild isolate and MMP strains. Natural variation and induced mutations that alter codons across *pot-2* are shown along with the telomere-length estimates for all strains. (A) A schematic illustrating the *pot-2* genomic region is shown. The dark gray region represents the part of the genome encoding the OB-fold domain. Purple regions represent untranslated regions. (B) Strains that harbor the alternative (non-reference) allele are plotted by telomere length on the y-axis and genomic position on the x-axis. Both synonymous and nonsynonymous variants are labeled. Variants resulting in a nonsynonymous coding change are bolded. The blue line indicates the median telomere-length value for wild isolates. The color of boxplots and markers indicates variants from the same haplotypes. (C) Boxplot of natural isolate distribution of telomere lengths. Blue lines within the center of each box represent the median while the box represents the IQR from the 25th–75th percentile. Whiskers extend to 1.5× the IQR above and below the box. Plotted points represent individual strains. (D) Telomere length is plotted on the y-axis as in (B), but strains do not share mutations because strains harbor unique collections of induced alleles. The blue line indicates median telomere length for the MMP population. (E) Boxplot of the distribution of telomere lengths in the MMP is shown. Boxplot follows same conventions as in (C). N2 telomere length in our population was estimated to be 16.9 kb, whereas median telomere length in MMP was estimated to be 4.94 kb. This disparity is likely caused by differences in library preparation, sequencing platform, and data processing.

Examination of Tajima's D at the *pot-2* locus yielded no conspicuous signature, though the characteristic high linkage disequilibrium of *C. elegans* makes gene-focused tests challenging in this species (Figure S13). Furthermore, the haplotypes that contain this variant are rare (Figure S14) and not geographically restricted (Figure S15). Like the measurements of organismal fitness and lack of correlation with telomere-length differences, the population genetic test of neutrality indicates that the observed variation in *pot-2* is not under strong selective pressure. Together, these results suggest that natural variation in telomere length plays a limited role in modifying whole-organism phenotypes in *C. elegans*.

## Discussion

In this study, we report the identification of a QTL on the right arm of chromosome II containing a variant within the gene

*pot-2* that contributes to differences in telomere length of *C. elegans* wild isolates. To date, no connection of *pot-2* to natural variation in telomere lengths has been described. Several lines of evidence support the F68I allele of *pot-2* as the variant modulating telomere lengths. First, others have shown previously that loss of *pot-2* results in progressive telomere lengthening in the laboratory strain background (Raices *et al.* 2008; Shtessel *et al.* 2013). Second, the F68I variant is the only SNV in *pot-2* that correlates with long telomeres. This variant falls within the OB fold of POT-2, and our examination of strain telomere lengths within the MMP shows enrichment of mutations from long-telomere strains found within the OB-fold domain. Third, OB folds are known to interact with single-stranded nucleic acids, and TelSeq telomere-length estimates of wild isolates and randomly mutagenized laboratory strains show that mutation or variation of the OB-fold domain reduces function and causes long telomeres, as we also observed in the

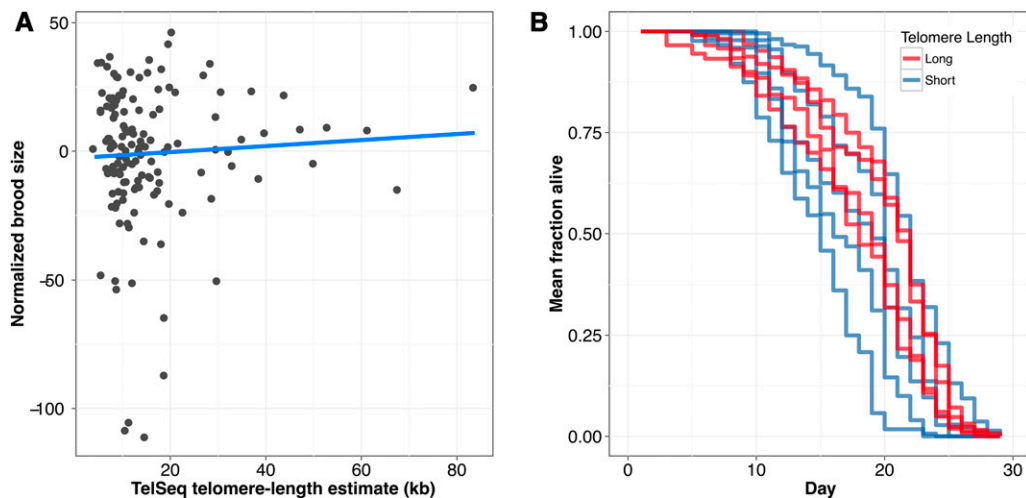


**Figure 6** Fitness traits are not associated with telomere length. (A) Normalized brood sizes (x-axis) of 152 wild isolates are plotted against the telomere-length estimates from those same strains (y-axis). The blue line indicates a linear fit of the data. However, the correlation is not significant ( $\rho = -0.062$ ,  $P = 0.463$ ). (B) Survival curves of nine wild isolates with long and short telomeres. Lines represent aggregate survival curves of three replicates. Survival among long and short telomere-length strains is not significantly different ( $P = 0.517$ ; Mantel–Cox analysis).

*pot-2(tm1400)* deletion strain. Moreover, this amino acid change could plausibly alter the function of the OB fold within *POT-2*. Nucleic acid recognition of OB folds occurs through a variety of molecular interactions, including aromatic stacking (Theobald *et al.* 2003). A change from phenylalanine to isoleucine would eliminate a potential aromatic stacking interaction and presumably reduce the binding affinity and function of *POT-2*. It would be interesting to determine if natural variation in either of the OB-fold domains of hPOT1 contribute to the natural variation in telomere lengths among diverse individuals in the human population.

We wondered why additional genes involved in the regulation of telomeres were not identified from our study of telomere lengths across wild isolates and mutagenized laboratory strains. Homologs for both telomerase and shelterin complex components are found in *C. elegans* (Stein *et al.* 2001). We identified natural variation in *trt-1* but only in the highly diverged strains ECA36 and QX1211. These rare alleles are removed from the GWA mapping because we require allele frequencies to be greater than 5%. Laboratory mutants in *trt-1* have short telomeres (Cheung *et al.* 2006; Meier *et al.* 2006), but we do not see enrichment of *trt-1* mutations in the MMP collection for short or long telomeres. *C. elegans* contains orthologous genes for two of the six shelterin complex members, hPOT1 and RAP1 (Harris *et al.* 2009). Four *C. elegans* genes with homology to hPOT1 have been identified (*mrt-1*, *pot-1*, *pot-2*, and *pot-3*) (Raices *et al.* 2008; Meier *et al.* 2009), and *C. elegans rap-1* is homologous to human RAP1 (Raices *et al.* 2008; Meier *et al.* 2009). The genes *rap-1* and *pot-3* had no variants or only rare variants, respectively. All of the other homologous genes contained variants in 5% or more of the wild isolates. None of these genes mapped by GWA besides *pot-2*, and none of the mutations in these genes were enriched in short- or long-telomere strains from the MMP collection. Perhaps shorter telomere strains are less fit and do not survive well in the wild or during the growth of mutant MMP strains. These results suggest that long telomeres are likely of limited consequence compared to short telomeres in natural settings. Additionally, because TelSeq provides an average estimate of

telomere length, it is possible for the variance of telomere lengths to increase without affecting average length estimates. For this reason, we might not detect a QTL at *pot-1*, which has been previously reported to result in longer but more heterogeneous telomeres (Raices *et al.* 2008).

Our observation that considerable telomere-length variation in the wild isolate population exists allowed us to directly test whether variation in telomere length contributes to organismal fitness. We did not see any correlation between telomere length and offspring production, suggesting that fitness in wild strains is not related to telomere length. In contrast to findings in human studies, we did not identify a relationship between telomere length and longevity. Our results confirm past findings that telomere length is not associated with longevity in a small number of *C. elegans* wild isolates or laboratory mutants (Raices *et al.* 2005). Although the effects of telomere length on longevity have been observed in a well controlled study of the gene *hrp-1* on isogenic populations in the laboratory (Joeng *et al.* 2004), this study differs from our results in wild isolates. The different genetic backgrounds of wild isolates could further complicate a connection of telomere length to longevity because of variable modifier loci and definitely noisy longevity assays. Even though we did not identify a correlation between telomere length and either longevity or offspring production under laboratory conditions, our study suggests a limited role for telomeres in postmitotic cells. Furthermore, the population genetic results do not strongly support evidence of selection on *pot-2* variants.

In summary, this study demonstrates that a variant in *pot-2* likely contributes to phenotypic differences in telomere length among wild isolates of *C. elegans*. The absence of evidence for selection on the alternative alleles at the *pot-2* locus and the lack of strong effects on organismal fitness traits suggest that differences in telomere length do not substantially affect individuals at least under laboratory growth conditions. Additionally, our study demonstrates the ability to extract and to use phenotypic information from sequence data. A number of approaches can be employed to examine other dynamic components of the genome, including mitochondrial and

ribosomal DNA copy numbers, the mutational spectrum, or codon biases. These traits present a unique opportunity to identify how genomes differ among individuals and the genetic variants underlying those differences.

## Acknowledgments

We thank Joshua Bloom and members of the Andersen laboratory for critical comments on this manuscript. We also thank M. Barkoulas, T. B elicaud, D. Bourc his, N. Callemeyn-Torre, S. Carvalho, J. Dumont, L. Fr ezal, C.-Y. Kao, L. Lokmane, I. Ly, K. Ly, A. Paaby, J. Riksen, and G. Wang for isolating new wild *C. elegans* strains. The National Bioresource Project provided the FX1400 strain, and Wormbase data made a variety of analyses possible. This work was supported by a National Institutes of Health R01 subcontract to E.C.A. (GM-107227), the Chicago Biomedical Consortium with support from the Searle Funds at the Chicago Community Trust, and an American Cancer Society Research Scholar grant to E.C.A. (127313-RSG-15-135-01-DD), along with support from the Cell and Molecular Basis of Disease training grant (T32GM008061) to S.Z. and from the National Science Foundation Graduate Research Fellowship (DGE-1324585) to D.E.C.

## Literature Cited

- Andersen, E. C., J. P. Gerke, J. A. Shapiro, J. R. Crissman, R. Ghosh *et al.*, 2012 Chromosome-scale selective sweeps shape *Caenorhabditis elegans* genomic diversity. *Nat. Genet.* 44: 285–290.
- Andersen, E. C., J. S. Bloom, J. P. Gerke, and L. Kruglyak, 2014 A Variant in the Neuropeptide Receptor *npr-1* is a Major Determinant of *Caenorhabditis elegans* Growth and Physiology. *PLoS Genet.* 10: e1004156.
- Andersen, E. C., T. C. Shimko, J. R. Crissman, R. Ghosh, J. S. Bloom *et al.*, 2015 A Powerful New Quantitative Genetics Platform, Combining *Caenorhabditis elegans* High-Throughput Fitness Assays with a Large Collection of Recombinant Strains. *G3 (Bethesda)* 5: 911–920.
- Armanios, M., J.-L. Chen, Y.-P. C. Chang, and R. A. Brodsky, A. Hawkins *et al.*, 2005 Haploinsufficiency of telomerase reverse transcriptase leads to anticipation in autosomal dominant dyskeratosis congenita. *Proc. Natl. Acad. Sci. USA* 102: 15960–15964.
- Barri re, A., and M.-A. F elix, 2005 Natural variation and population genetics of *Caenorhabditis elegans* (December 26, 2005), *Wormbook*, ed. The *C. elegans* Research Community WormBook, doi/10.1895/wormbook.1.43.1, <http://www.wormbook.org>.
- Blackburn, E. H., 1991 Structure and function of telomeres. *Nature* 350: 569–573.
- Bolger, A. M., M. Lohse, and B. Usadel, 2014 Trimmomatic: A flexible trimmer for Illumina sequence data. *Bioinformatics* 30: 2114–2120.
- Boyd, W. A., S. J. McBride, J. R. Rice, D. W. Snyder, and J. H. Freedman, 2010 A high-throughput method for assessing chemical toxicity using a *Caenorhabditis elegans* reproduction assay. *Toxicol. Appl. Pharmacol.* 245: 153–159.
- Broer, L., V. Codd, D. R. Nyholt, J. Deelen, M. Mangino *et al.*, 2013 Meta-analysis of telomere length in 19,713 subjects reveals high heritability, stronger maternal inheritance and a paternal age effect. *Eur. J. Hum. Genet.* 21: 1163–1168.
- Browning, B. L., and S. R. Browning, 2016 Genotype Imputation with Millions of Reference Samples. *Am. J. Hum. Genet.* 98: 116–126.
- Cawthon, R. M., 2009 Telomere length measurement by a novel monochrome multiplex quantitative PCR method. *Nucleic Acids Res.* 37: 1–7.
- Cheng, C., L. Shtessel, M. M. Brady, and S. Ahmed, 2012 *Caenorhabditis elegans* POT-2 telomere protein represses a mode of alternative lengthening of telomeres with normal telomere lengths. *Proc. Natl. Acad. Sci. USA* 109: 7805–7810.
- Cheung, I., M. Schertzer, A. Baross, A. M. Rose, P. M. Lansdorp *et al.*, 2004 Strain-specific telomere length revealed by single telomere length analysis in *Caenorhabditis elegans*. *Nucleic Acids Res.* 32: 3383–3391.
- Cheung, I., M. Schertzer, A. Rose, and P. M. Lansdorp, 2006 High incidence of rapid telomere loss in telomerase-deficient *Caenorhabditis elegans*. *Nucleic Acids Res.* 34: 96–103.
- Cingolani, P., A. Platts, L. L. Wang, M. Coon, T. Nguyen *et al.*, 2012 A program for annotating and predicting the effects of single nucleotide polymorphisms, SnpEff: SNPs in the genome of *Drosophila melanogaster* strain w 1118; iso-2; iso-3. *Fly (Austin)* 6: 80–92.
- Codd, V., C. P. Nelson, E. Albrecht, M. Mangino, J. Deelen *et al.*, 2013 Identification of seven loci affecting mean telomere length and their association with disease. *Nat. Genet.* 45: 422–427e2.
- Deng, Y., S. S. Chan, and S. Chang, 2008 Telomere dysfunction and tumour suppression: the senescence connection. *Nat. Rev. Cancer* 8: 450–458.
- Ding, Z., M. Mangino, A. Aviv, T. Spector, and R. Durbin, 2014 Estimating telomere length from whole genome sequence data. *Nucleic Acids Res.* 42: 1–4.
- Edgar, R. C., 2004 MUSCLE: Multiple sequence alignment with high accuracy and high throughput. *Nucleic Acids Res.* 32: 1792–1797.
- Endelman, J. B., 2011 Ridge Regression and Other Kernels for Genomic Selection with R Package rrBLUP. *Plant Genome J.* 4: 250–255.
- F elix, M.-A., and C. Braendle, 2010 The natural history of *Caenorhabditis elegans*. *Curr. Biol.* 20: R965–R969.
- Flynn, R. L., and L. Zou, 2010 Oligonucleotide/oligosaccharide-binding fold proteins: a growing family of genome guardians. *Crit. Rev. Biochem. Mol. Biol.* 45: 266–275.
- Frenck, R. W., Jr., E. H. Blackburn, and K. M. Shannon, 1998 The rate of telomere sequence loss in human leukocytes varies with age. *Proc. Natl. Acad. Sci. USA* 95: 5607–5610.
- Fulcher, N., A. Teubenbacher, E. Kerdaffrec, A. Farlow, M. Nordborg *et al.*, 2014 Genetic Architecture of Natural Variation of Telomere Length in *Arabidopsis thaliana*. *Genetics* 199: 625–635.
- Gatbonton, T., M. Imbesi, M. Nelson, J. M. Akey, D. M. Ruderfer *et al.*, 2006 Telomere length as a quantitative trait: Genome-wide survey and genetic mapping of telomere length-control genes in yeast. *PLoS Genet.* 2: e35.
- Gordon, A., and G. J. Hannon, 2010 FASTX Toolkit, FASTQ/A short-reads pre-processing tools. Hannon Lab. Available at: [http://hannonlab.cshl.edu/fastx\\_toolkit](http://hannonlab.cshl.edu/fastx_toolkit). Accessed January, 2016.
- Griffith, J. D., L. Comeau, S. Rosenfield, R. M. Stansel, A. Bianchi *et al.*, 1999 Mammalian telomeres end in a large duplex loop. *Cell* 97: 503–514.
- Harley, C. B., H. Vaziri, C. M. Counter, and R. C. Allsopp, 1992 The telomere hypothesis of cellular aging. *Exp. Gerontol.* 27: 375–382.
- Harris, T. W., I. Antoshechkin, T. Bieri, D. Blasiar, and J. Chan *et al.*, 2009 Wormbase: A comprehensive resource for nematode research. *Nucleic Acids Res.* 38: D463–D467.
- Heidinger, B. J., J. D. Blount, W. Boner, K. Griffiths, N. B. Metcalfe *et al.*, 2012 Telomere length in early life predicts lifespan. *Proc Natl Acad Sci USA* 109: 1743–1748.
- Hornsby, P. J., 2007 Telomerase and the aging process. *Exp. Gerontol.* 42: 575–581.
- Joeng, K. S., E. J. Song, K.-J. Lee, and J. Lee, 2004 Long lifespan in worms with long telomeric DNA. *Nat. Genet.* 36: 607–611.
- Jones, A. M., A. D. Beggs, L. Carvajal-Carmona, and S. Farrington, A. Tenesa *et al.*, 2012 TERC polymorphisms are associated



- both with susceptibility to colorectal cancer and with longer telomeres. *Gut*. 61: 248–254.
- Kwan, E. X., E. Foss, L. Kruglyak, and A. Bedalov, 2011 Natural polymorphism in BUL2 links cellular amino acid availability with chronological aging and telomere maintenance in yeast. *PLoS Genet.* 7: e1002250.
- Lack, J. B., C. M. Cardeno, M. W. Crepeau, W. Taylor, R. B. Corbett-Detig *et al.*, 2015 The Drosophila Genome Nexus: A Population Genomic Resource of 623 Drosophila melanogaster Genomes, Including 197 from a Single Ancestral Range Population. *Genetics* 199: 1229–1241.
- De Lange, T., 2010 How shelterin solves the telomere end-protection problem. *Cold Spring Harb. Symp. Quant. Biol.* 75: 167–177.
- Lei, M., E. R. Podell, and T. R. Cech, 2004 Structure of human POT1 bound to telomeric single-stranded DNA provides a model for chromosome end-protection. *Nat. Struct. Mol. Biol.* 11: 1223–1229.
- Levy, D., S. L. Neuhausen, S. C. Hunt, M. Kimura, S.-J. Hwang *et al.*, 2010 Genome-wide association identifies OBFC1 as a locus involved in human leukocyte telomere biology. *Proc. Natl. Acad. Sci. USA* 107: 9293–9298.
- Levy, M. Z., R. C. Allsopp, A. B. Futcher, C. W. Greider, and C. B. Harley, 1992 Telomere end-replication problem and cell aging. *J. Mol. Biol.* 225: 951–960.
- Li, H., 2011 A statistical framework for SNP calling, mutation discovery, association mapping and population genetical parameter estimation from sequencing data. *Bioinformatics* 27: 2987–2993.
- Li, H., and R. Durbin, 2009 Fast and accurate short read alignment with Burrows-Wheeler transform. *Bioinformatics* 25: 1754–1760.
- Liti, G., S. Haricharan, F. A. Cubillos, A. L. Tierney, S. Sharp *et al.*, 2009 Segregating YKU80 and TLC1 alleles underlying natural variation in telomere properties in wild yeast. *PLoS Genet.* 5: e1000659.
- Mackay, T. F., S. Richards, E. A. Stone, A. Barbadilla, J. F. Ayroles *et al.*, 2012 The Drosophila melanogaster Genetic Reference Panel. *Nature* 482: 173–178.
- Malik, H. S., W. D. Burke, and T. H. Eickbush, 2000 Putative telomerase catalytic subunits from Giardia lamblia and Caenorhabditis elegans. *Gene* 251: 101–108.
- Marrone, A., A. Walne, and I. Dokal, 2005 Dyskeratosis congenita: Telomerase, telomeres and anticipation. *Curr. Opin. Genet. Dev.* 15: 249–257.
- McCarthy, M. I., G. R. Abecasis, L. R. Cardon, D. B. Goldstein, and J. Little *et al.*, 2008 Genome-wide association studies for complex traits: consensus, uncertainty and challenges. *Nat. Rev. Genet.* 9: 356–369.
- McEachern, M. J., A. Krauskopf, and E. H. Blackburn, 2000 Telomeres and their control. *Annu. Rev. Genet.* 34: 331–358.
- McGrath, P. T., M. V. Rockman, M. Zimmer, H. Jang, E. Z. Macosko *et al.*, 2009 Quantitative Mapping of a Digenic Behavioral Trait Implicates Globin Variation in C. elegans Sensory Behaviors. *Neuron* 61: 692–699.
- McMurdie, P. J., and S. Holmes, 2013 Phyloseq: An R Package for Reproducible Interactive Analysis and Graphics of Microbiome Census Data. *PLoS One* 8: e61217.
- Meier, B., I. Clejan, Y. Liu, M. Lowden, A. Gartner *et al.*, 2006 trt-1 is the Caenorhabditis elegans catalytic subunit of telomerase. *PLoS Genet.* 2: 187–197.
- Meier, B., L. J. Barber, L. Shtessel, S. J. Boulton, A. Gartner *et al.*, 2009 The MRT-1 nuclease is required for DNA crosslink repair and telomerase activity in vivo in Caenorhabditis elegans. *EMBO J.* 28: 3549–3563.
- Noble, L. M., A. S. Chang, D. McNelis, M. Kramer, M. Yen *et al.*, 2015 Natural Variation in plep-1 Causes Male-Male Copulatory Behavior in C. Elegans. *Curr. Biol.* 25: 2730–2737.
- O’Sullivan, R. J., and J. Karlseder, 2010 Telomeres: protecting chromosomes against genome instability. *Nat. Rev. Mol. Cell Biol.* 11: 171–181.
- Paradis, E., J. Claude, and K. Strimmer, 2004 APE: Analyses of phylogenetics and evolution in R language. *Bioinformatics* 20: 289–290.
- Poon, S. S., U. M. Martens, R. K. Ward, and P. M. Lansdorp, 1999 Telomere length measurements using digital fluorescence microscopy. *Cytometry* 36: 267–278.
- R Development Core Team, 2013 R: A Language and Environment for Statistical Computing. R Foundation for Statistical Computing, Vienna, Austria.
- Raices, M., H. Maruyama, A. Dillin, and J. Karlseder, 2005 Uncoupling of longevity and telomere length in C. elegans. *PLoS Genet.* 1: 295–301.
- Raices, M., R. E. Verdun, S. A. Compton, C. I. Haggbloom, J. D. Griffith *et al.*, 2008 C. elegans Telomeres Contain G-Strand and C-Strand Overhangs that Are Bound by Distinct Proteins. *Cell* 132: 745–757.
- Rockman, M. V., and L. Kruglyak, 2009 Recombinational landscape and population genomics of Caenorhabditis elegans. *PLoS Genet.* 5: e1000419.
- Rozen, S., and H. J. Skaletsky, 2000 Primer3 on the WWW for General Users and for Biologist Programmers, pp. 365–386 in *Bioinformatics Methods and Protocols*, edited by S. Misener and S. A. Krawetz. Methods Mol. Biol. TM 132. Humana Press.
- Samassekou, O., M. Gadj, R. Drouin, and J. Yan, 2010 Sizing the ends: Normal length of human telomeres. *Ann. Anat.* 192: 284–291.
- Seo, B., C. Kim, M. Hills, S. Sung, H. Kim *et al.*, 2015 Telomere maintenance through recruitment of internal genomic regions. *Nat. Commun.* 6: 8189.
- Shimko, T. C., and E. C. Andersen, 2014 COPASutils: An R Package for Reading, Processing, and Visualizing Data from COPAS Large-Particle Flow Cytometers. *PLoS One* 9: e111090.
- Shtessel, L., M. R. Lowden, C. Cheng, M. Simon, K. Wang *et al.*, 2013 Caenorhabditis elegans POT-1 and POT-2 repress telomere maintenance pathways. *G3 (Bethesda)* 3: 305–313.
- Soerensen, M., M. Thinggaard, M. Nygaard, S. Dato, Q. Tan *et al.*, 2012 Genetic variation in TERT and TERC and human leukocyte telomere length and longevity: A cross-sectional and longitudinal analysis. *Aging Cell* 11: 223–227.
- Stein, L., P. Sternberg, R. Durbin, J. Thierry-Mieg, and J. Spieth, 2001 WormBase: network access to the genome and biology of Caenorhabditis elegans. *Nucleic Acids Res.* 29: 82–86.
- Sterken, M. G., L. B. Snoek, J. E. Kammenga, and E. C. Andersen, 2015 The laboratory domestication of Caenorhabditis elegans. *Trends Genet.* 31: 224–231.
- Stiemagel, T., 2006 Maintenance of C. elegans. *WormBook* 11: 1–11.
- The 1000 Genomes Project Consortium, 2012 An integrated map of genetic variation from 1,092 human genomes. *Nature* 491: 56–65.
- Theobald, D. L., R. M. Mitton-Fry, and D. S. Wuttke, 2003 Nucleic Acid Recognition by OB-Fold Proteins. *Annu Rev Biophys Biomol Struct.* 32: 115–133.
- Thompson, O., M. Edgley, P. Strasbourger, S. Flibotte, B. Ewing *et al.*, 2013 The million mutation project: A new approach to genetics in Caenorhabditis elegans. *Genome Res.* 23: 1749–1762.
- Vulliamy, T., A. Marrone, R. Szydlo, A. Walne, P. J. Mason *et al.*, 2004 Disease anticipation is associated with progressive telomere shortening in families with dyskeratosis congenita due to mutations in TERC. *Nat. Genet.* 36: 447–449.
- Watson, J. D., 1972 Origin of concatemeric T7 DNA. *Nat. New Biol.* 239: 197–201.
- Weigel, D., and R. Mott, 2009 The 1001 genomes project for Arabidopsis thaliana. *Genome Biol.* 10: 107.
- Wicks, S. R., R. T. Yeh, W. R. Gish, R. H. Waterston, and R. H. Plasterk, 2001 Rapid gene mapping in Caenorhabditis elegans using a high density polymorphism map. *Nat. Genet.* 28: 160–164.
- Wicky, C., A. M. Villeneuve, N. Lauper, L. Codourey, H. Tobler, and F. Müller, 1996 Telomeric repeats (TTAGGC)<sub>n</sub> are sufficient for chromosome capping function in Caenorhabditis elegans. *Proc. Natl. Acad. Sci. USA* 93: 8983–8988.

Communicating editor: V. Reinke

# GENETICS

Supporting Information

[www.genetics.org/lookup/suppl/doi:10.1534/genetics.116.191148/-/DC1](http://www.genetics.org/lookup/suppl/doi:10.1534/genetics.116.191148/-/DC1)

## **The Genetic Basis of Natural Variation in *Caenorhabditis elegans* Telomere Length**

Daniel E. Cook, Stefan Zdraljevic, Robyn E. Tanny, Beomseok Seo, David D. Riccardi,  
Luke M. Noble, Matthew V. Rockman, Mark J. Alkema, Christian Braendle, Jan E. Kammenga,  
John Wang, Leonid Kruglyak, Marie-Anne Félix, Junho Lee, and  
Erik C. Andersen

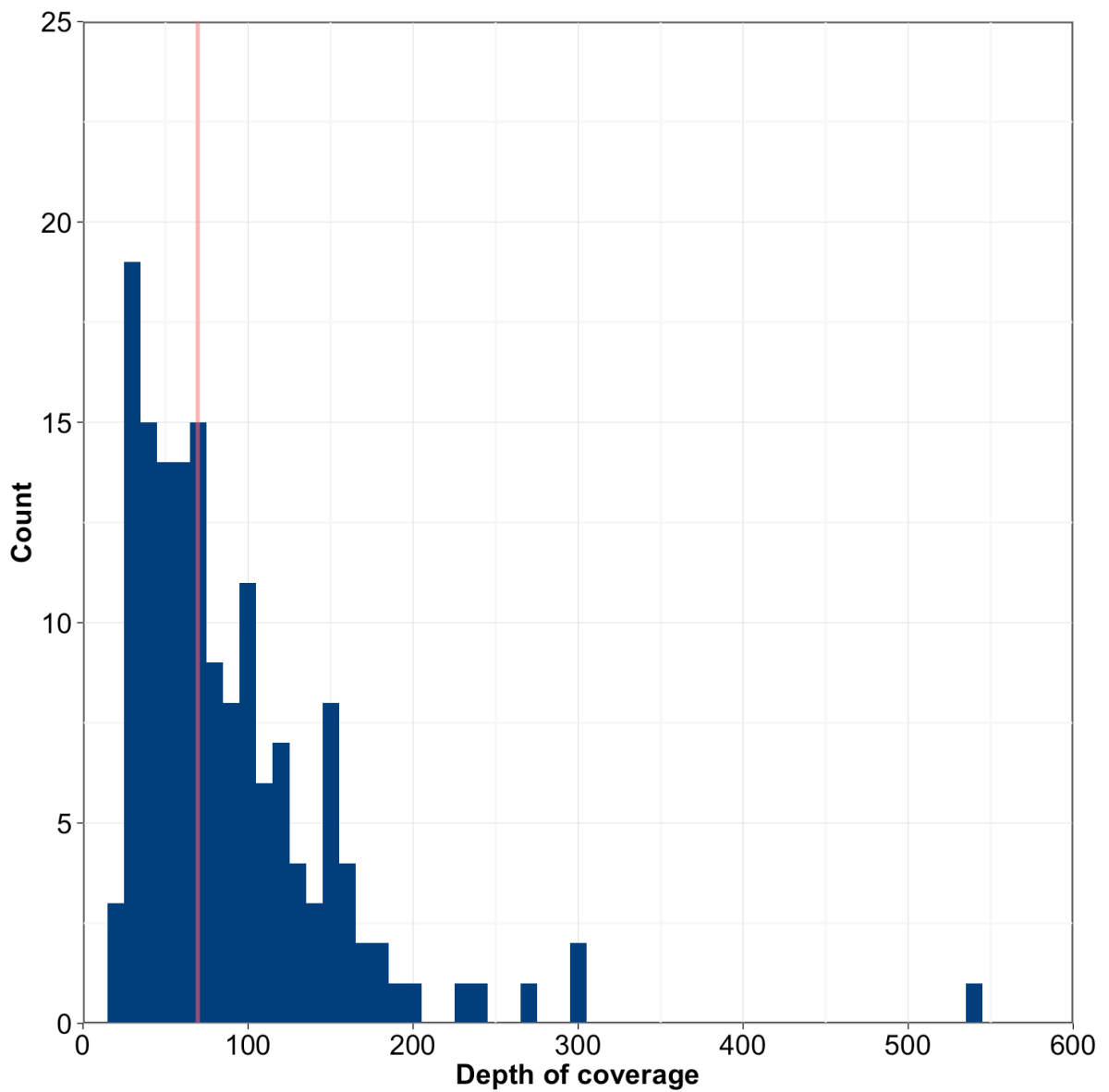


**Figure S1:** Distribution of the depth of coverage among 152 isotypes The distribution of depth of coverage for 152 isotypes is shown. The red line indicates median depth of coverage: 70x.

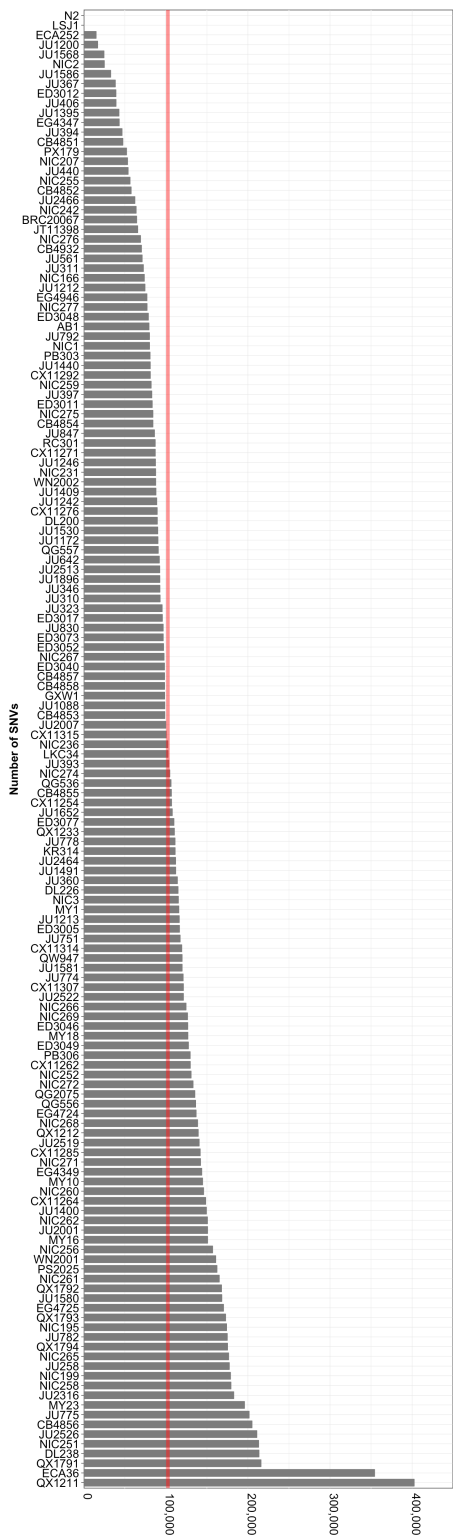


**Figure S2:** Distribution of number of variant sites as compared to the WS245 reference genome  
 Number of single nucleotide variants (SNVs) is plotted on the x-axis for each isotope (y-axis).



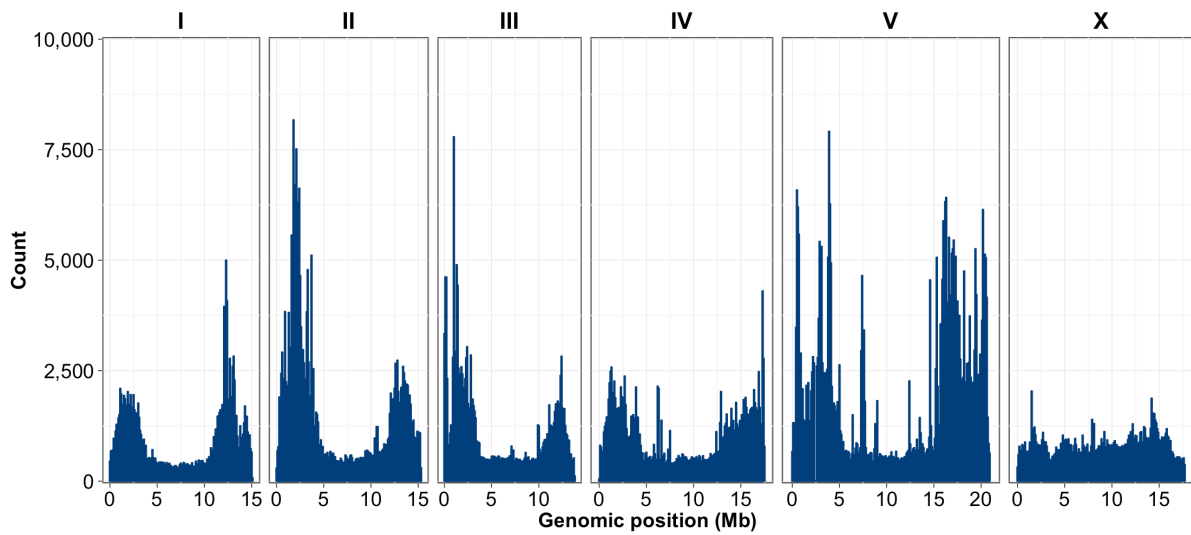


**Figure S3** Distribution of SNVs by chromosome

The number of SNV sites identified from the 152 isotypes relative to the N2 strain were calculated in 100 kb bins and plotted by genomic position (x-axis). The density of SNVs is greater on chromosome arms than in centers.

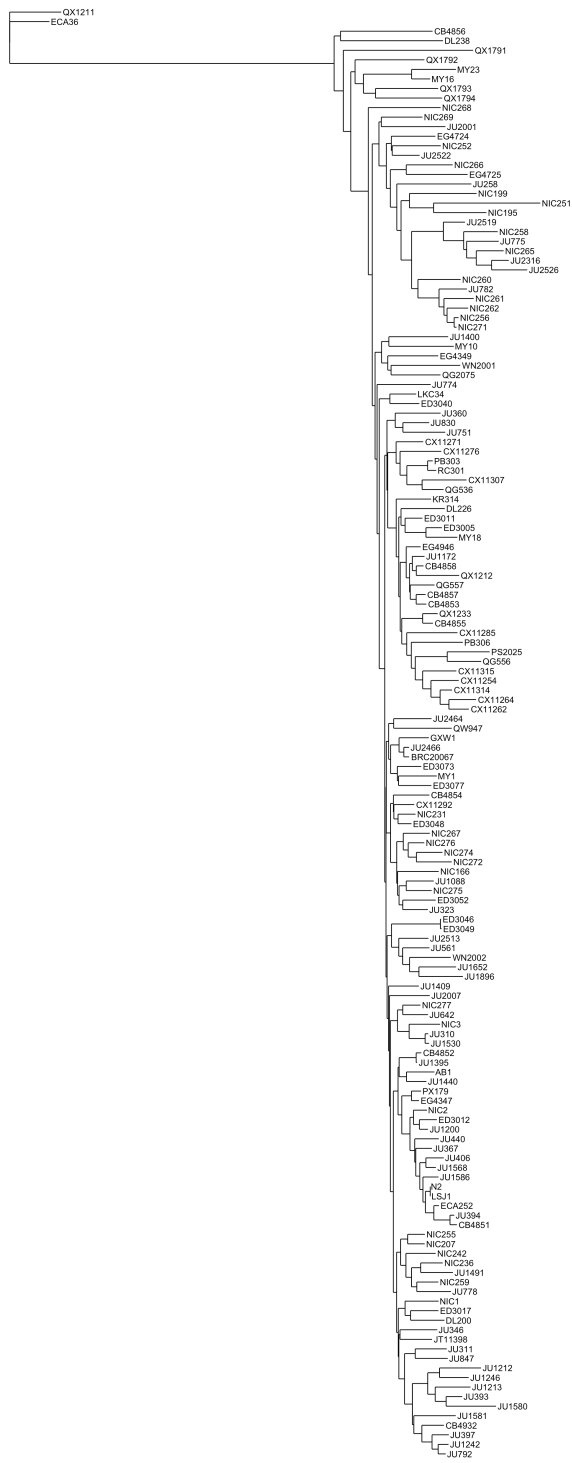
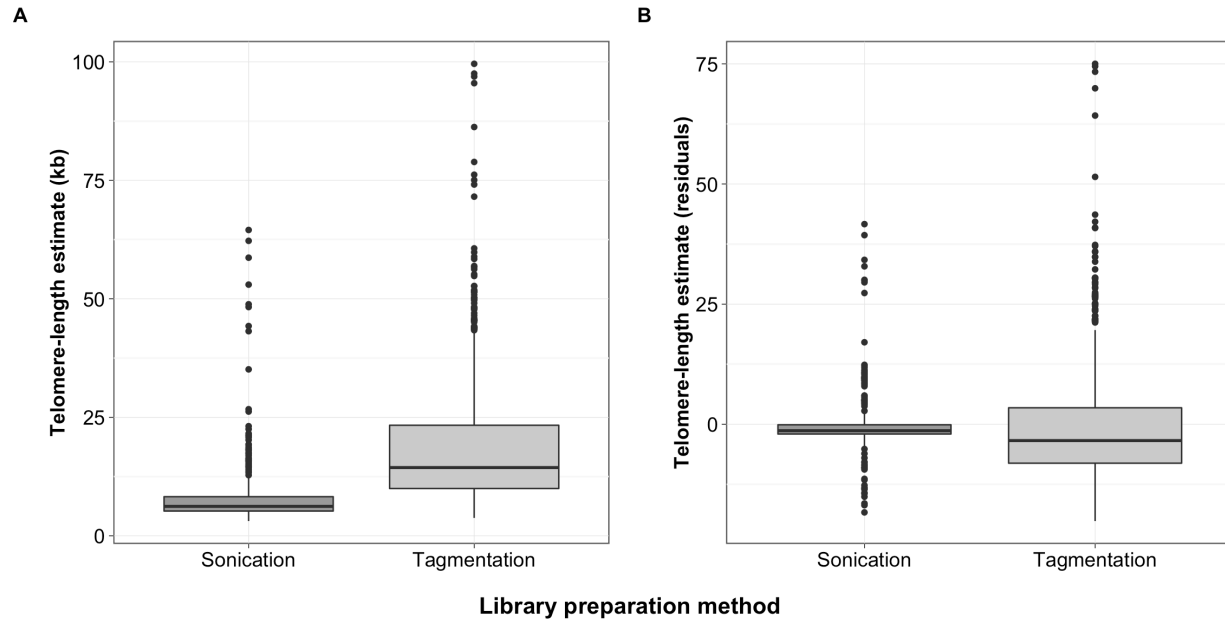
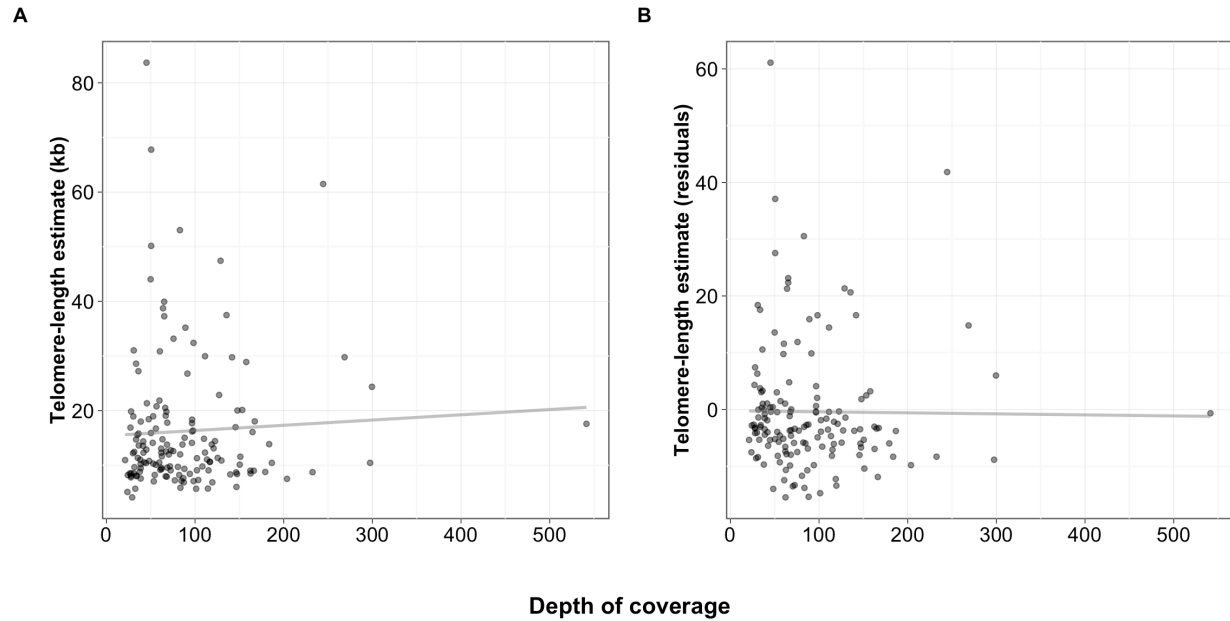


Figure S4: Similarity tree of 152 *C. elegans* isotypes.



**Figure S5** TelSeq differences by DNA fragmentation method

Differences in TelSeq length estimates based on DNA fragmentation method shown as boxplots. Dark lines within the center of each box represent the median, and the box represents the interquartile range (IQR) from the 25<sup>th</sup>-75<sup>th</sup> percentile. Whiskers extend to 1.5x the IQR above and below the box. Points represent estimates beyond 1.5x the IQR. **(A)** Uncorrected TelSeq length estimates are plotted on the y-axis by DNA fragmentation method. **(B)** Residual telomere length estimates are plotted by DNA fragmentation method.



**Figure S6:** Lack of a significant correlation between depth of coverage and TelSeq length estimate

Scatterplots of the depths of coverage for isotypes on the x-axis plotted against **(A)** the TelSeq telomere-length estimates ( $\rho = 0.045$ ,  $p = 0.576$ ). **(B)** Depths of coverage are plotted against the residuals of the TelSeq length estimates after adjusting for sequencing center (run) and sequencing library ( $\rho = -0.134$ ,  $p = 0.097$ ).



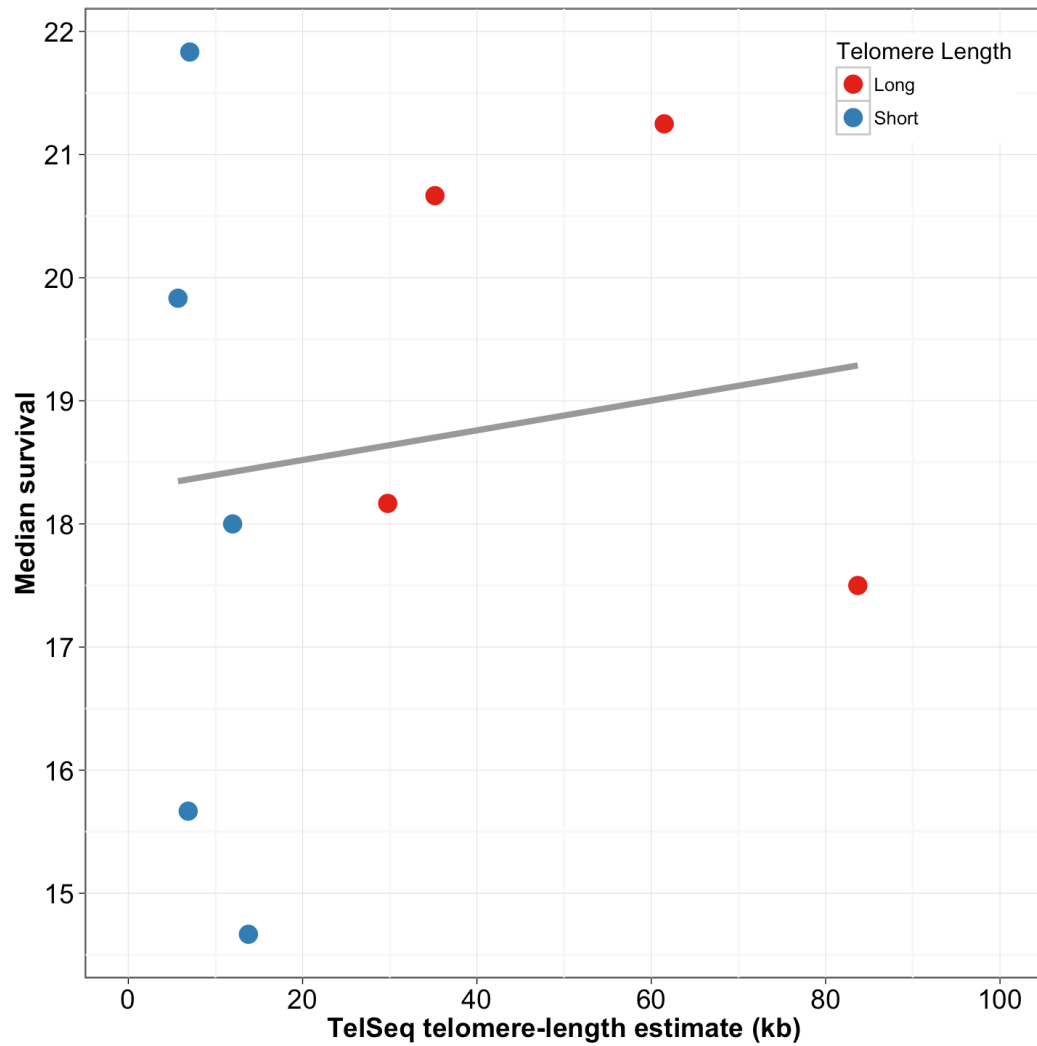
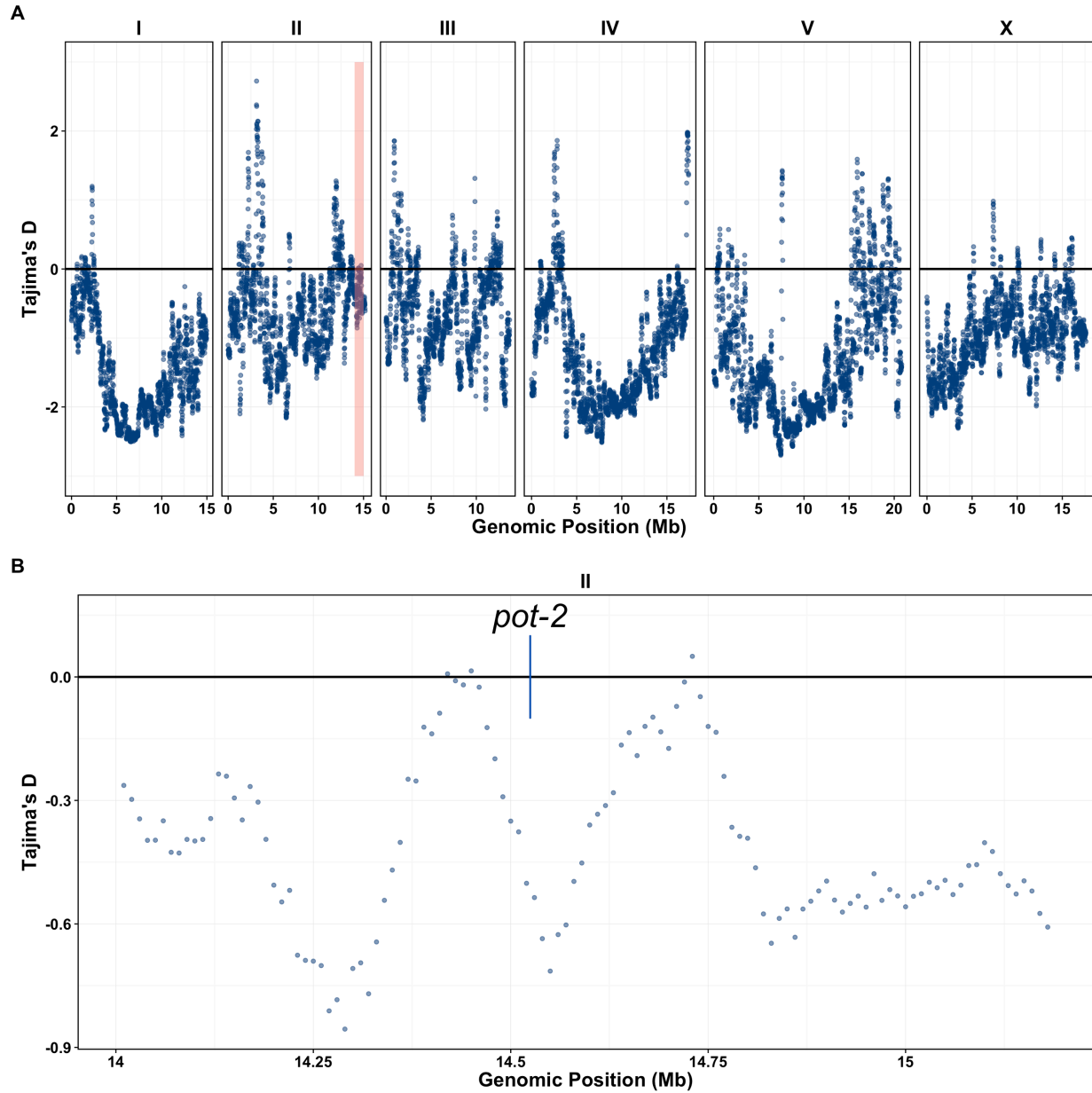


Figure S7: Longevity is not associated with telomere length

Median day of survival (x-axis) is plotted against the estimated telomere length (y-axis). The correlation is not significant ( $\rho = 0.05$ ,  $p = 0.91$ ).



**Figure S8:** Tajima's D does not support evidence of selection at the *pot-2* locus

Tajima's D values were calculated genome wide (window-size = 100,000, step-size = 10,000). **(A)** Distribution of Tajima's D values plotted by genomic position. The red box represents the region shown in panel **(B)** that contains the *pot-2* locus.

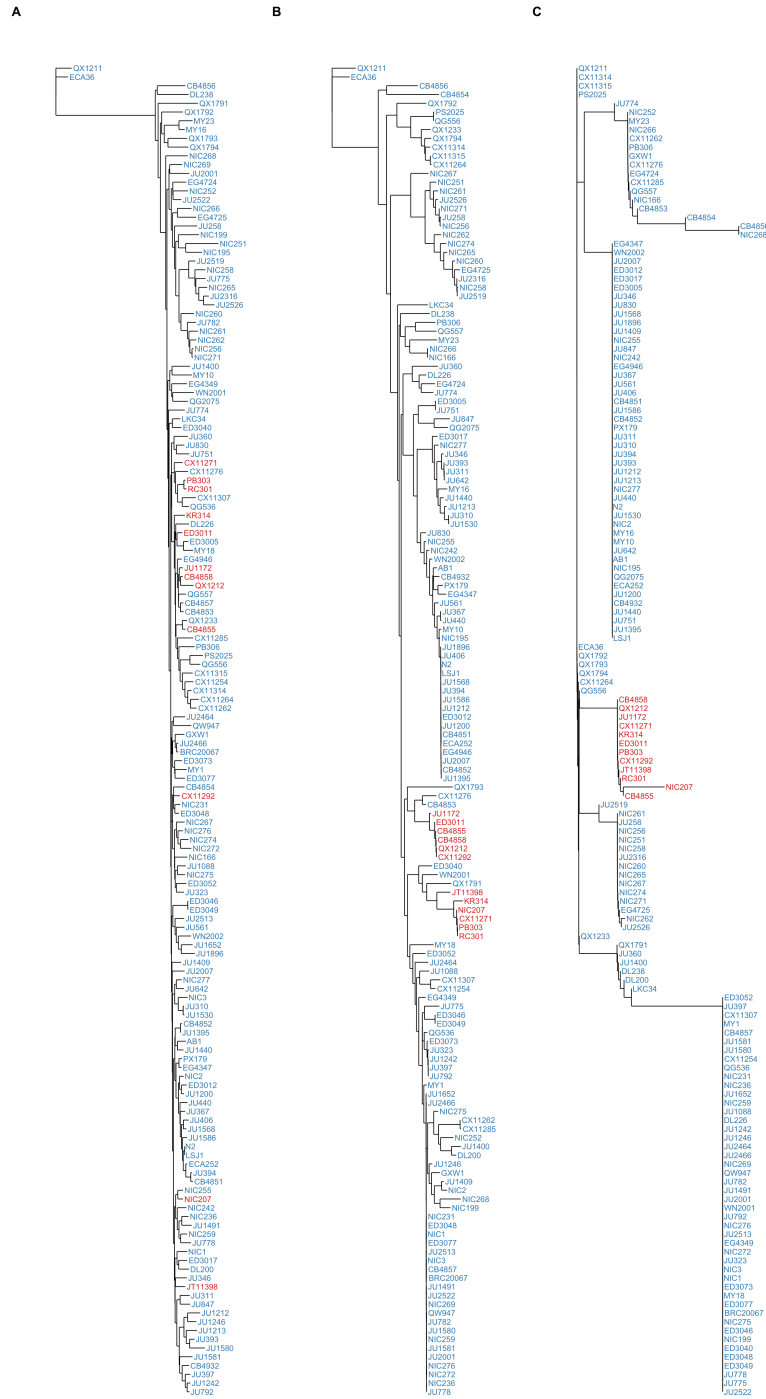


**Figure S9:** Similarity trees of genome, chromosome II, and the *pot-2* locus

Isotypes are colored by their POT-2 F68I variant status. F=Blue, I=Red. Trees were generated from SNVs **(A)** genome-wide, **(B)** using SNVs located on the right arm of chromosome II (13Mb to the terminus), or **(C)** using SNVs located within the *pot-2* region (II:14,524,173-14,525,111).

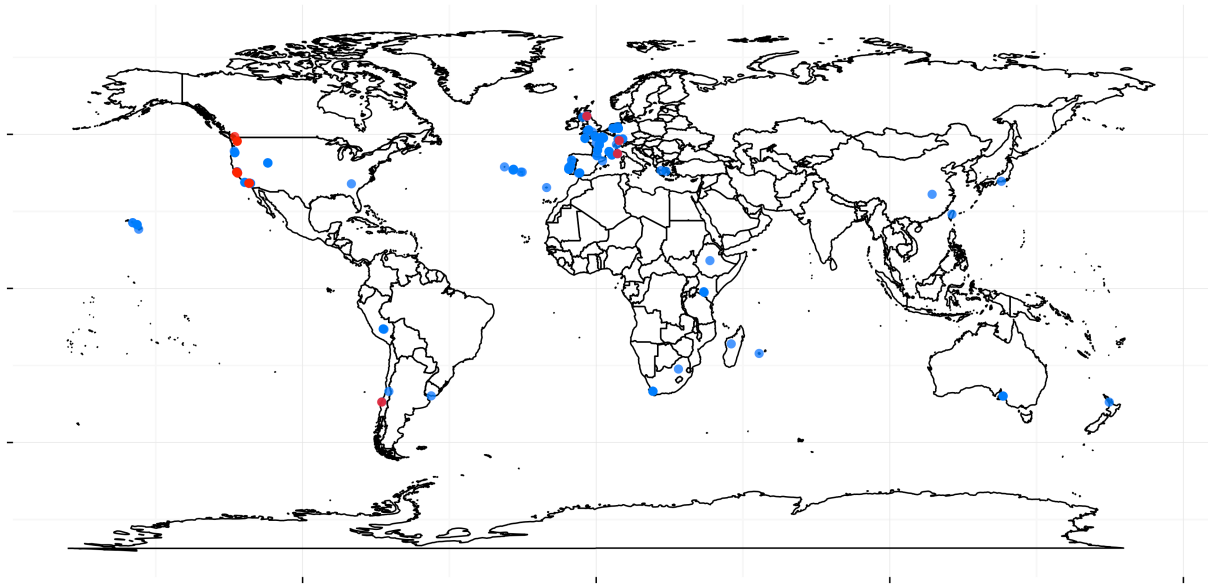


**Figure S10:** Strains with the F68I variant are not found in similar geographic locations

The isolation location of the reference strain for each isotype is plotted. Location markers are colored according to the status of the F68I allele for that isotype (F = Blue, I = Red).

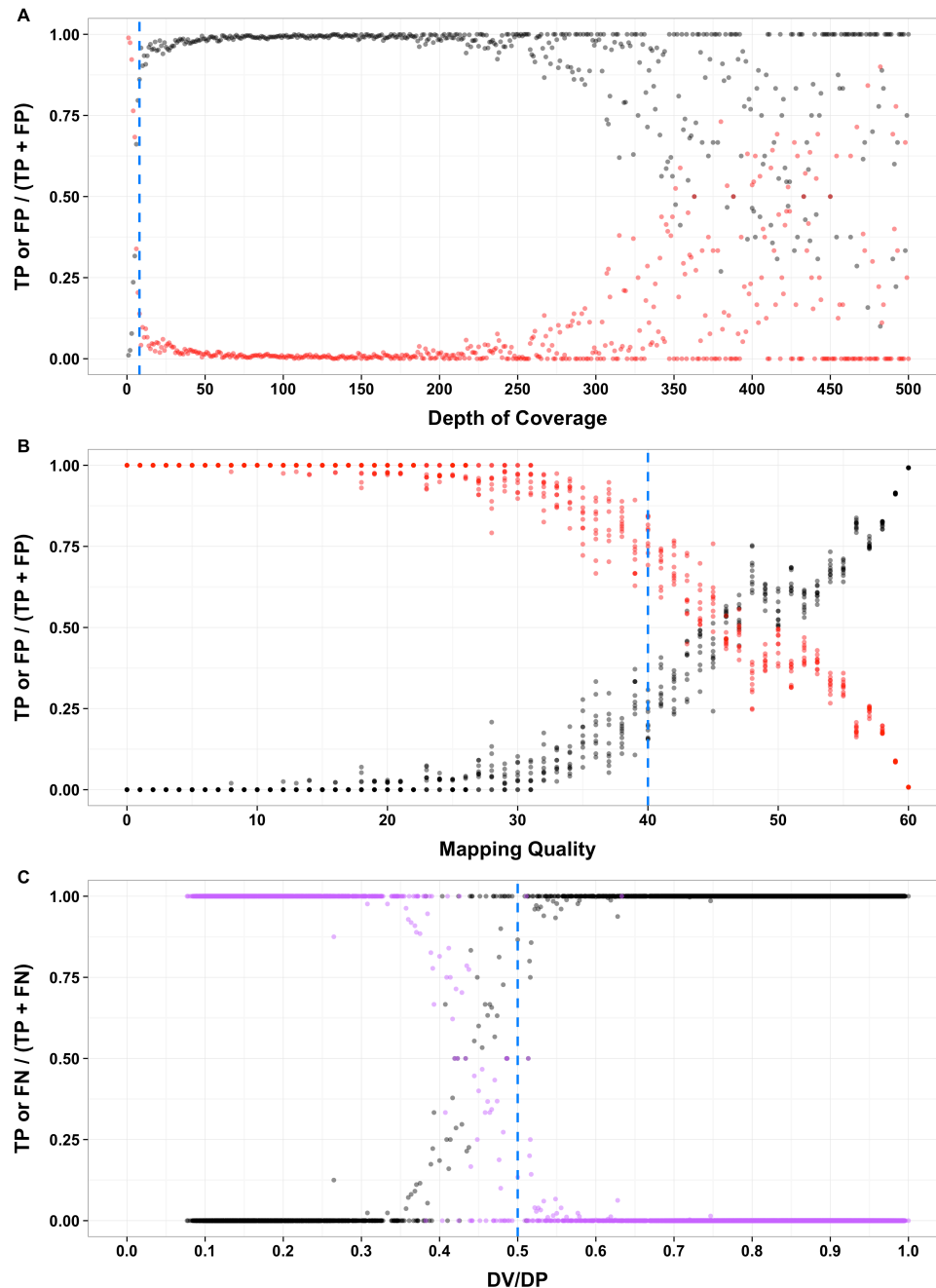


**Figure S11:** Evaluation of variant-calling parameters from a simulated variant data set

True positive (TP; black), false positive (FP; red), and false negative (FN; purple) rates across variant parameters suggest appropriate filter thresholds. The y-axis is the rate is the rate of TP compared with either FP or FN variants. The rate of TP and FP or FN is plotted on the x-axis across (A) depth of coverage, (B), mapping quality, or (C) the number of high-quality non-reference bases (DV) over depth (DP) at a given site.



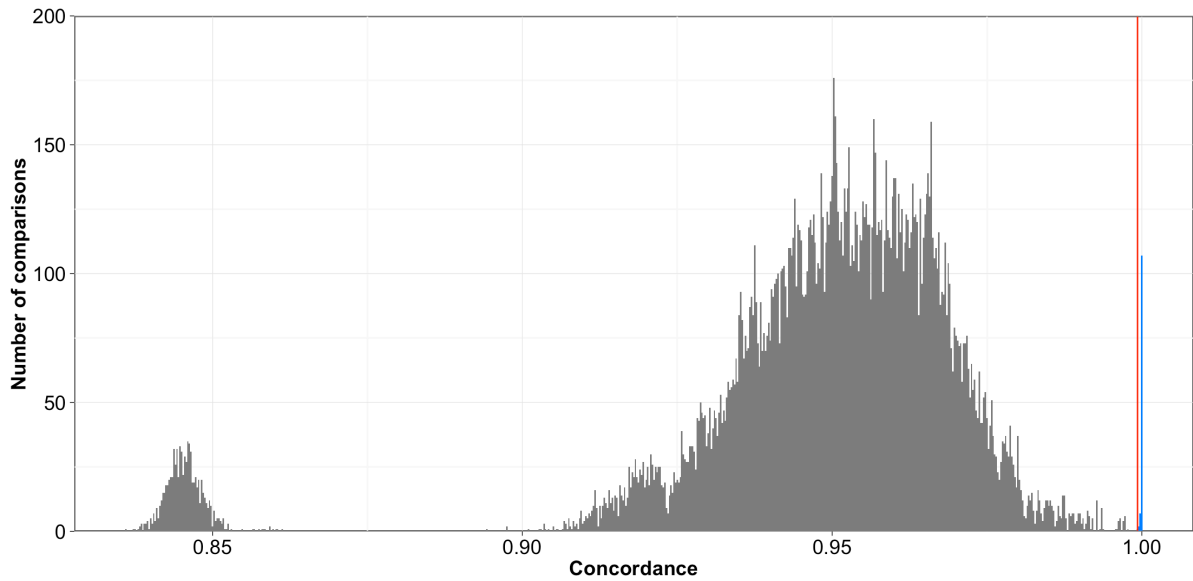


**Figure S12:** Pairwise SNV concordance among isotypes

Pairwise SNV concordances among all strains were assessed by comparing SNV calls between pairs of strains. Concordance is plotted on the x-axis. The red line indicates the cutoff used to assign isotypes (0.9993). Strains with concordances above this level were classified as isotypes and are colored in blue.

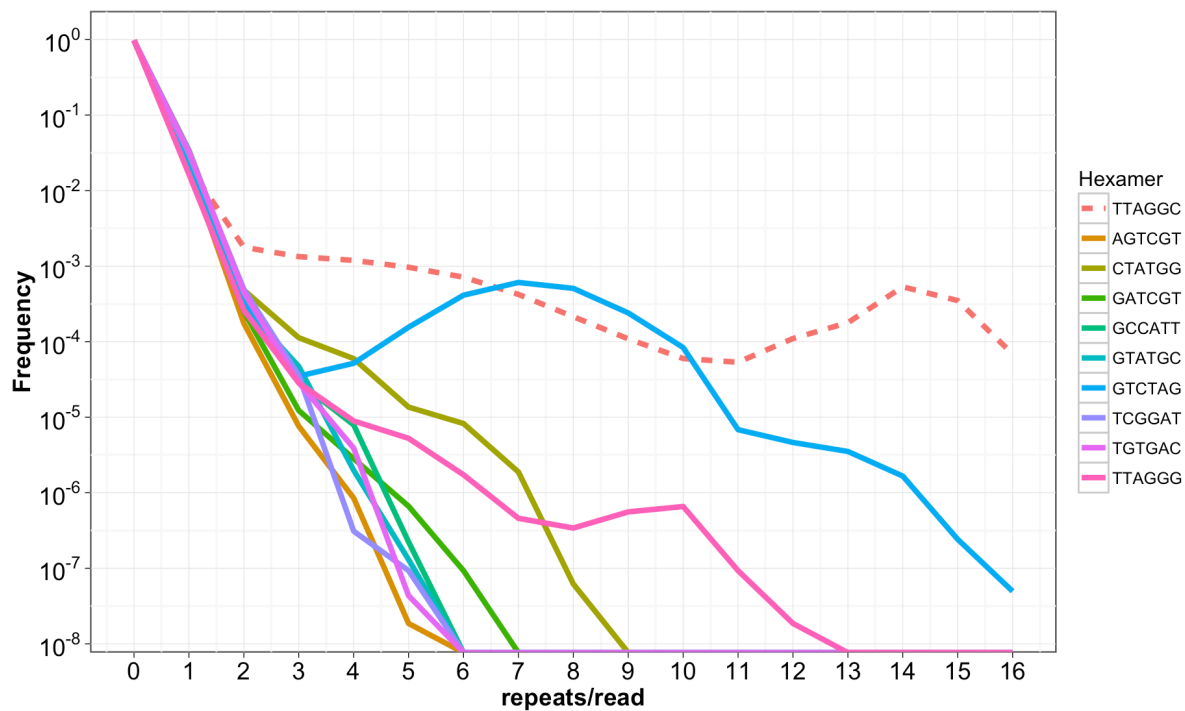


**Figure S13:** Frequency of hexamers in short reads generated from the N2 strain

The frequency of non-cyclical permutations of the telomeric hexamer is plotted on the y-axis against the number of hexamer repeats per read on the x-axis. The line color indicates the hexamer. The dashed line represents the telomeric hexamer repeat in *C. elegans*.

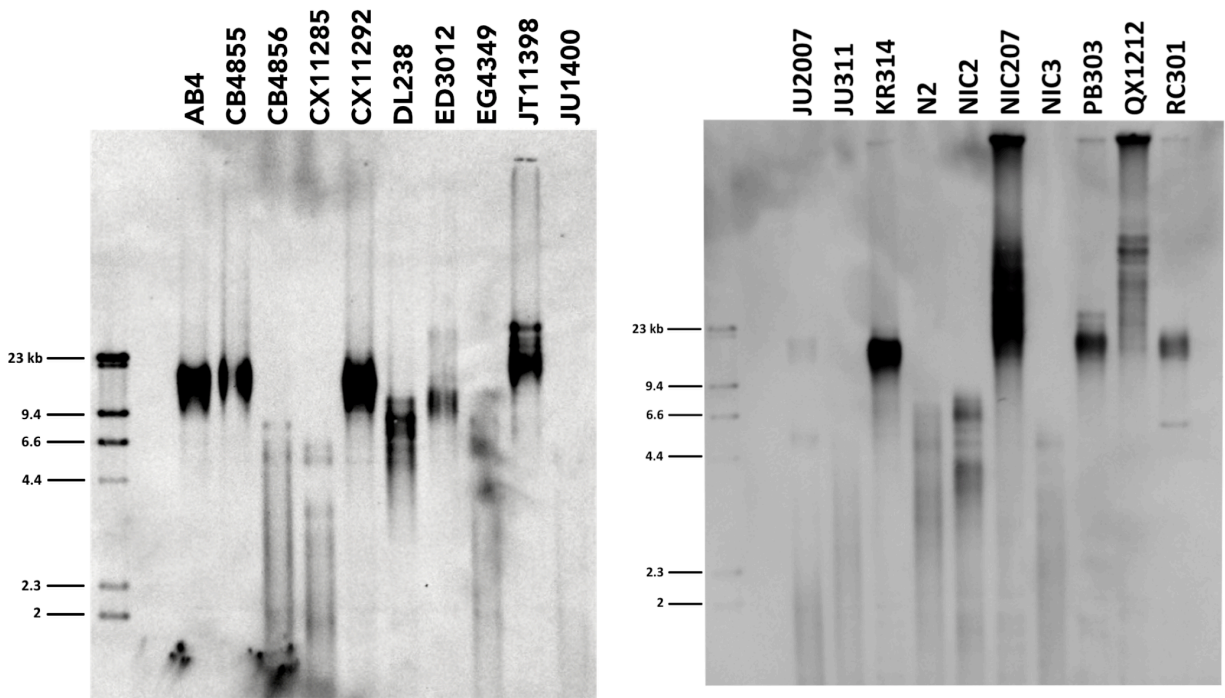


**Figure S14:** Terminal restriction fragment (TRF) Southern blot Analysis

Terminal restriction fragment analysis was performed on a subset of wild strains to evaluate the accuracy of TelSeq telomere-length estimates. Genomic DNA from wild isolates was separated by pulsed-field gel electrophoresis. Equivalent amounts of DNA were loaded into each lane.

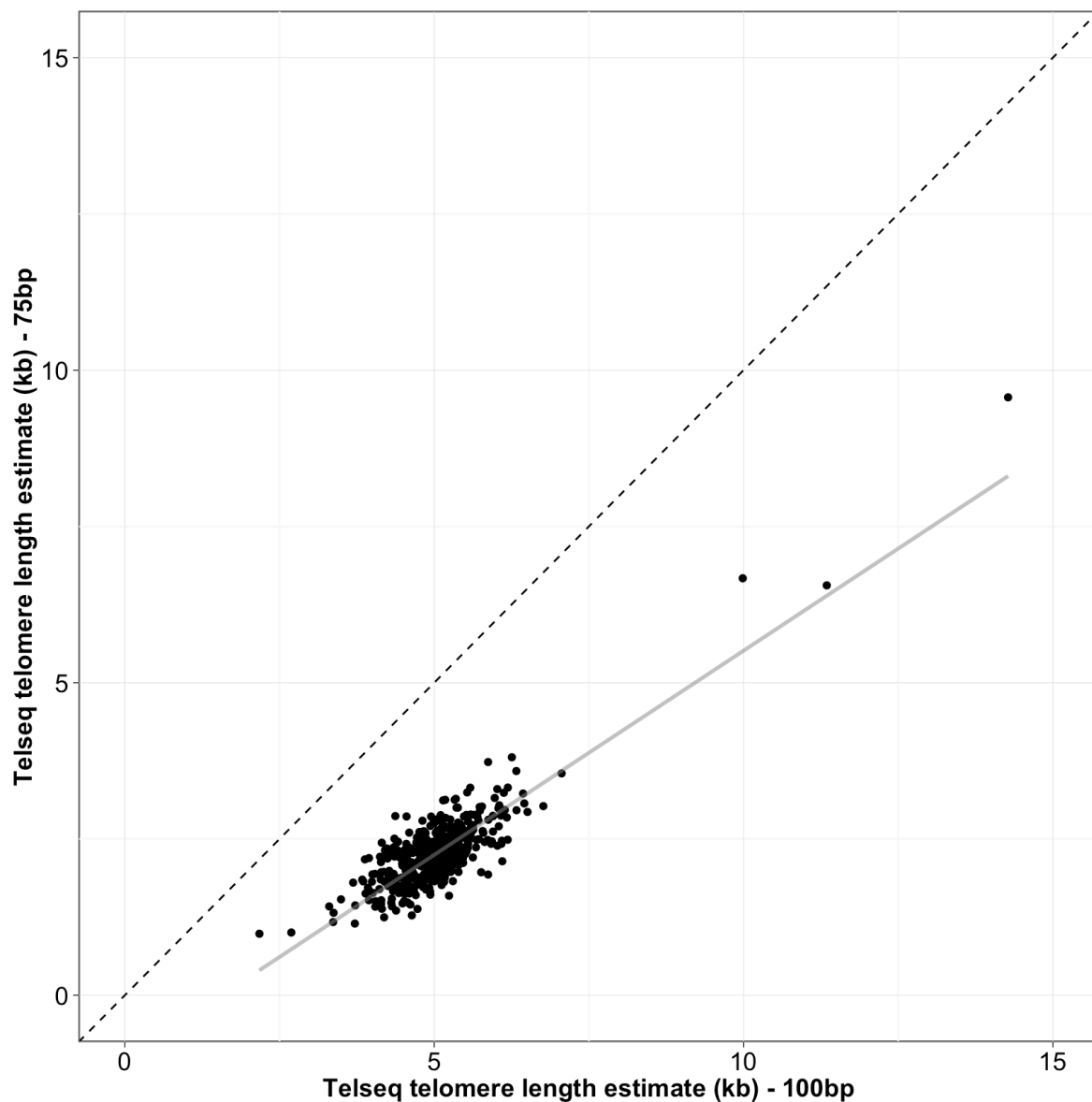


**Figure S15** Correcting MMP TelSeq estimates for differences in read length

TelSeq telomere-length estimates from 448 Million Mutation Project strains sequenced at 75 bp and 100 bp were used to develop a linear model for converting TelSeq estimates. This transformation enabled us to convert TelSeq estimates using sequence data from 75 bp runs. The correlation between 75 bp and 100 bp estimates was  $r^2 = 0.723$ .

File S1: Strain isotype grouping and collection information. (.zip, 9 KB)

Available for download as a .zip file at:

<http://www.genetics.org/lookup/suppl/doi:10.1534/genetics.116.191148/-/DC1/FileS1.zip>



File S2: TelSeq telomere length estimates among wild isolates. (.zip, 2 KB)

Available for download as a .zip file at:

<http://www.genetics.org/lookup/suppl/doi:10.1534/genetics.116.191148/-/DC1/FileS2.zip>

File S3: Telomere length measurements comparison. (.zip, 1 KB)

Available for download as a .zip file at:

<http://www.genetics.org/lookup/suppl/doi:10.1534/genetics.116.191148/-/DC1/FileS3.zip>

File S4: Genome-wide association mapping results. (.zip, 192 KB)

Available for download as a .zip file at:

<http://www.genetics.org/lookup/suppl/doi:10.1534/genetics.116.191148/-/DC1/FileS4.zip>

File S5: Correlations of variants within QTL on chromosome II. (.zip, 5 KB)

Available for download as a .zip file at:

<http://www.genetics.org/lookup/suppl/doi:10.1534/genetics.116.191148/-/DC1/FileS5.zip>

File S6: Summary of sequencing libraries and preparation. (.zip, 7 KB)

Available for download as a .zip file at:

<http://www.genetics.org/lookup/suppl/doi:10.1534/genetics.116.191148/-/DC1/FileS6.zip>



File S7: Rates of heterozygosity for different SNV calling methods. (.zip, 1 KB)

Available for download as a .zip file at:

<http://www.genetics.org/lookup/suppl/doi:10.1534/genetics.116.191148/-/DC1/FileS7.zip>

File S8: Summary of variant filters. (.zip, 1 KB)

Available for download as a .zip file at:

<http://www.genetics.org/lookup/suppl/doi:10.1534/genetics.116.191148/-/DC1/FileS8.zip>

File S9: Telomere hexamer locations across WS245. (.zip, 24 KB)

Available for download as a .zip file at:

<http://www.genetics.org/lookup/suppl/doi:10.1534/genetics.116.191148/-/DC1/FileS9.zip>

File S10: Telseq length estimates by sequencing run. (.zip, 20 KB)

Available for download as a .zip file at:

<http://www.genetics.org/lookup/suppl/doi:10.1534/genetics.116.191148/-/DC1/FileS10.zip>

File S11: *p*-values for enrichment test of protein coding genes. (.zip, 19 KB)

Available for download as a .zip file at:

<http://www.genetics.org/lookup/suppl/doi:10.1534/genetics.116.191148/-/DC1/FileS11.zip>